Drought-Induced Soil Carbon Dynamics in Subtropical Forests: Emergent Divergence from Model Structures

Fengfeng Du[1], LianJun Feng[1], Lingyan Zhou[2], Zhizhuang Gu[3], Yaqi Zhang[1], Zhenggang Du[1*], Xuhui Zhou[1]

[1]Northeast Asia ecosystem Carbon sink research Center (NACC), Key Laboratory of Sustainable Forest Ecosystem Management-Ministry of Education, School of Forestry, Northeast Forestry University, Harbin, 150040, China

[2]Shanghai Engineering Research Center of Sustainable Plant Innovation, Shanghai Botanical Garden, Shanghai, China

[3]Zhejiang Tiantong Forest Ecosystem National Observation and Research Station, School of Ecological and Environmental Sciences, East China Normal University, Shanghai, 200062, China

*Corresponding author. Email: zgdu@nefu.edu.cn

ABSTRACT

Accurately quantifying drought impacts on terrestrial carbon cycling is essential for advancing predictions of climate-carbon feedbacks. However, current biogeochemical models exhibit limited capability in simulating drought-induced transformations of soil organic carbon (SOC), particularly regarding microbial processes. Here, we conducted a systematic comparative evaluation of three prevailing SOC modeling structures, including conventional three-pool partitioning scheme (SM1), mineral and particulate-associated carbon partitioning scheme (SM2) and Michaelis-Menten regulated carbon-stabilization scheme (SM3), to elucidate their capacity in simulating soil carbon dynamics under decadal drought scenarios in a subtropical forest. We found divergent effects of drought in soil C input (SM1, 66%; SM2, 10%; SM3, -4%) and mean residence time (MRT; SM1, -31%; SM2, -14%; SM3, 65%), which lead to the predicted SOC substantial accumulation for both SM1 and SM3 (+39.5% and +56.9%, respectively) and moderate depletion (-6.1%) for SM2. Drought leads to a decrease in microbial carbon and an increase in POC, while the responses of other carbon pools vary across different models. These findings highlight critical model structural dependencies in simulating drought-affected soil carbon dynamics and emphasize the necessity for models to integrate microbial-physicochemical interactions for improved climate-carbon coupling projections.

Keywords: soil carbon stock, extreme drought, microbial enzyme activity, model comparison, data assimilation, traceability analysis.

删除了: The different C input directly affect the passive SOC (SM1) and mineral-associated organic carbon (SM2 and SM3). In comparison, the drought effects on passive SOC (SM1), microbe biomass (SM2) and MAOC (SM2 and SM3), lead to notable spread in MRT

设置了格式: 字体: (默认) Times New Roman, 小四

1 Introduction

Terrestrial ecosystems are facing increasing frequent stress from extreme drought which fundamentally alters plant-microbe-mineral interactions, serving as a key driver of carbon sequestration patterns (IPCC, 2023; Han et al., 2022; Choat et al., 2018; Hao et al., 2015). Initial drought exposure typically enhances soil organic carbon (SOC) stability via physicochemical protection mechanisms, such as reduced microbial decomposition from moisture limitation (Schimel, 2018), increased organo-mineral association due to soil contraction (Blankinship et al., 2016), and disrupted enzyme diffusion (Wu et al., 2025). However, plant-derived carbon inputs decline through productivity suppression driven by hydraulic failure (Choat et al., 2018) and carbon allocation shifts away from roots (Yin et al., 2021). Prolonged drought (e.g., >2 years) induces microbial adaptation strategies which may accelerate SOC loss (Barnard et al., 2013; Schimel et al., 2018). The shift toward filamentous fungal dominance enhances oxidative enzyme production, while necromass accumulation primes destabilization of mineral-associated carbon (Liang et al., 2020; Wang et al., 2024). However, predicting how terrestrial carbon storage responds to drought over decadal timescales remains a challenge, requiring the integration of long-term manipulative experiments with models capable of capturing drought-induced changes in plant-microbe-mineral interactions.

In most terrestrial ecosystem models, SOC is typically represented as discrete compartments defined by their turnover times (Krinner et al., 2005; Lawrence et al., 2019). Early modeling approaches, such as the single-pool model proposed by Jenny et al. (1941), treated SOC as a homogeneous system. Subsequent refinements led to the

删除了: l

删除了: which drives

批注 [JF1]: 标黄色的在参考文献处补上文献

删除了: a

删除了: i

删除了:

带格式的: 缩进: 首行缩进: 1.18 字符

development of multi-pool frameworks. For example, Campbell et al. (1978) categorized SOC into labile and stable organic matter. The TECO model further advanced this by partitioning SOC into three pools (fast, slow, and passive SOM) with different turnover rates (Xu et al., 2006; Du et al., 2017; Wan et al., 2025). Later developments incorporated greater complexity, such as separating recalcitrant fractions and accounting for physically protected organic matter, which decomposes more slowly than unprotected forms (Paul et al., 1978; Willard et al., 2024).

Theoretical advancements in soil organic matter (SOM) formation and decomposition improve the representation of SOC in land-surface and terrestrial ecosystem models (Basile-Doelsch et al., 2020; Si et al., 2023; Cotrufo et al., 2022; Sokol et al.,2019). Measured SOC fractions, such as particulate organic carbon (POC), mineral-associated organic carbon (MAOC) and dissolved organic carbon (DOC), have been proposed to link conceptual SOC pools (Lee et al., 2020). POC is typically considered as fragments of plant residues with a particle size > 53 μm, and it is more susceptible to external environment changes (Cotrufo et al., 2019; Benbi et al., 2014; Lugato et al., 2022). MAOC generally consists of microbial and plant-derived organo-mineral complexes rich in nutrients, typically < 53 μm, while also being associated with minerals and embedded in soil aggregates (Si et al., 2023; Hansen et al., 2024; Villarino et al., 2021). Some studies have revealed that models constrained by measurable SOC pools can provide more accurate estimation of model parameters thereby more accurate projections of SOC dynamics (Guo et al., 2022; Tao et al., 2024; Abramoff et al., 2022). Dissolved organic carbon (DOC), derived from living roots or

删除了： Despite these advancements, SOC pools remain conceptual constructs simulated via first-order kinetics. Importantly, the carbon content of individual pools cannot be empirically measured, model calibration relies solely on total SOC (Guo et al., 2022).

删除了: Doelsch

设置了格式: 突出显示

transformed from recalcitrant macromolecular organic matter, is approximately 2 to 3 times more efficient than litter in forming SOM (Sokol et al., 2019; Cotrufo et al., 2013). Moreover, the adsorption and desorption processes of DOC represent a key link in SOC decomposition (Camino-Serrano et al., 2018; Wu et al., 2014). Consequently, incorporating DOC and its interaction with SOC into models represents a crucial advance.

Soil organic matter decomposition is a stepwise process in which microbes secrete extracellular enzymes to catalyze the substrate, converting SOM into assimilable subunits (Caldwell et al., 2005; Szejgis et al., 2024). Extensive manipulative experiments reveal that short-term drought limits microbial activities and substrate decomposition rates by inducing osmotic stress and constraining substrate diffusion (Honeker et al., 2024; Citerne et al., 2021). In contrast, long-term drought alters microbial community structure and carbon utilization patterns (Hueso et al., 2012; Preece et al., 2019; Wang et al., 2024). As catalysts of decomposition, microbial enzyme activities are impacted by drought (Sardans et al., 2010; Stursová et al., 2012; Wu et al., 2025). For example, drought significantly reduces the activities of β-glucosidase, acid phosphatase and polyphenol oxidase, although certain oxidases remain unaffected by soil moisture (Su et al., 2020a; Allison et al., 2023; Ficken & Warren., 2019). In recent years, microbial models, which focus on the process of microbial decomposition, have become increasingly incorporated in process-based ecological models (Moorhead et al., 2006; Lawrence et al., 2009; Allison et al., 2010; Huang et al., 2018).

删除了: soil organic matter

删除了:

删除了: Soil organic matter

带格式的: 缩进: 首行缩进: 1.18 字符

删除了: soil organic matter

删除了: Ma et al., 2024;

删除了: Ficken et al., 2019

删除了: However, most microbial models focus only on simulating carbon dynamics under warming and nitrogen deposition scenarios (Luo et al., 2020; Knorr et al., 2005; Eastman et al., 2024), while studies investigating drought effects on SOC dynamics and microbial decomposition remain scarce. Consequently, incorporating microbial enzymes to terrestrial ecosystem model are necessary to elucidate microbial regulation of soil carbon responses to drought.

Despite these advancements, a critical knowledge gap remains: how structural uncertainty, fundamentally different assumptions about carbon stabilization, leads to divergent projections of SOC response to decadal drought which refers to continuously reduced approximately 70% of natural rainfall sustained for over a decade (Su et al., 2020a). Traditional three-pool models feature conceptually unmeasurable carbon pools, and predictions of SOC rely solely on parameterization of total SOC (Guo et al., 2022), which obscures the responses of different carbon fractions (POC, MAOC, DOC) to drought and may lead to substantial errors in long-term projections. Furthermore, current models rarely explicitly represent the direct regulation of SOC by specific microbial enzymes and the effects of prolonged drought (Luo et al., 2020; Knorr et al., 2005; Eastman et al., 2024). Emerging frameworks that incorporate measurable fractions or explicit microbial enzyme kinetics (Michaelis-Menten dynamics) offer the potential to mechanistically represent the processes. However, these approaches differ fundamentally in their representation of carbon stabilization and decomposition, and no systematic evaluation has compared their performance against long-term drought experimental data. Such a comparison is essential, as the choice of model structure may not only influence predictive accuracy but also shape our mechanistic understanding of whether drought induces SOC loss or stabilization over decadal timescales.

In this study, we evaluate three SOC modeling schemes with increasing complexity, including conventional three-pool partitioning scheme (SM1), mineral and particulate-associated carbon partitioning scheme (SM2) and Michaelis-Menten regulated carbon-stabilization scheme (SM3). Using observational data from long-term drought

删除了:
删除了: alternative SOC model
带格式的: 缩进: 首行缩进: 1.77 字符
删除了: es
删除了: with contrasting
删除了: or convergent
删除了: ,
设置了格式: 非突出显示
删除了: ref??
删除了:
设置了格式: 字体颜色: 红色
删除了:
带格式的: 缩进: 首行缩进: 1.18 字符
删除了: [SM1]
删除了: [SM2]
删除了: [SM3]

experiments, we assess their validity and predictive performance. Our study addresses two key questions: (1) how does decadal drought affect SOC storage in subtropical forests? (2) do different model structures yield consistent drought impacts on SOC projections?

2 Materials and methods

2.1 Site description and data source

The Zhejiang Tiantong Forest Ecosystem National Field Scientific Observation and Research Station (28°48′N, 121°47′E, 163 m a.s.l) is located in Ningbo, Zhejiang Province. The site has a typical mid-subtropical monsoon climate with relatively distinct seasons. Summers are generally mild and rainy, while winters are dry with little precipitation. The annual average temperature in the study area is approximately 16.2 ℃. The annual average precipitation and evaporation are 1384 mm and 1320 mm, respectively, and the relative air humidity can reach 85%. The predominant soil type in the site is red-yellow soil and soil parent materials are mainly weathered products of some granite and sedimentary rocks. The soil texture consists of sand (6.8%), silt (55.5%), and clay (37.7%), with a pH ranging from about 4.4 to 5.1 (Gao et al., 2014). The vegetation type in the study area is typical subtropical evergreen broad-leaved forest, with secondary forests being the main vegetation type. The forest stocking density is approximately 3400 trees·hm^{-2}. The drought experiment was established in July 2013, which is composed of three experimental plots with similar terrain, vegetation type and stand condition (Su et al., 2020b).

删除了: $^{-2}$

设置了格式: 上标

删除了:

The forcing datasets used in this study span from 2014 to 2022, including photosynthetically active radiation (PAR), leaf area index (LAI), air temperature (Ta), relative humidity of air (RH), soil temperature (Ts) and moisture content of soil (SWC). These data were mainly measured by the station meteorological observation device. The above-ground biomass data of plants were mainly estimated by allometric growth equation. The C content of litter was determined by potassium dichromate oxidation method. Soil total organic carbon and its physical and chemical properties were measured by elemental analyzer. Microbial biomass carbon was determined by chloroform fumigation. DOC was determined by hot water extraction and element analyzer (Zhou et al., 2013). Soil enzyme activities were determined by microplate enzyme assay (Saiya-Cork et al., 2002; Su et al., 2020b) and was expressed by substrate conversion per gram of dry soil per hour. The soil respiration rate was measured using the *LI-COR 8100 portable system* (LI-COR. Inc., Lincoln, NE, USA) between 9 a.m. and 1 p.m. on 1 - 2 sunny days per month, and accumulated the data on daily scale.

2.2 Model description

All three soil models are coupled to a common vegetation submodule (Fig. 1). The vegetation model simulates photosynthesis and the flow of GPP within vegetation carbon pools. The photosynthesis process is implemented using the FBEM model, which is driven by leaf area index, photosynthetically active radiation, air temperature, and air relative humidity, detailed information can be found in Wu et al (2009). Vegetation is divided into three carbon pools: foliage, fine roots, and wood. A portion of GPP is returned to the atmosphere as respiration, while the remaining Net Primary

删除了: ,

设置了格式: 突出显示

Productivity (NPP) is allocated as a carbon source to the three vegetation carbon pools. Carbon transferred from these three vegetation pools is directed to two litter pools: metabolic litter and structural litter. The decomposed carbon from the litter pools serves as the source for soil carbon pools, which is then input into three soil modules. In this way, we ensure that the three soil modules share the same meteorological forcing data and SOC input, thereby facilitating a better analysis of differences arising from model structure, detailed descriptions can be found in Du et al (2025). In SM1, SOC is divided into three pools, including (1) a microbial pool with fast turnover; (2) a slow (chemically protected) pool, and (3) a passive (physically protected) pool (Xu et al., 2006; Du et al., 2015). In SM2, SOC is divided into four pools (Si et al., 2023), including (1) a dissolved organic carbon pool (DOC), which is converted from organic matter with high molecular weight and difficult to decompose. Microbes can utilize DOC and release CO_2 (Allison et al., 2010; Lawrence et al., 2009); (2) a microbial pool; (3) a particulate organic carbon pool (POC), and (4) a mineral- associated organic carbon (MAOC). SM3 is an extension of SM2 that incorporates three enzyme components: β-1, 4-glucosidase (BG), polyphenol oxidase (PPO), and cellobiohydrolase (CBH). These three enzymes provide a parsimonious yet functionally representative set for capturing drought effects on SOC decomposition (Chen et al., 2018). BG and CBH are primarily involved in the depolymerization of cellulose and labile carbon compounds, while PPO is associated with the oxidation of more recalcitrant substrates such as lignin-like compounds (Su et al., 2020b). Together, these enzymes capture the rate-limiting steps of both labile and resistant carbon

删除了: which requires identical environmental drivers and provides the same input da

删除了: ta

删除了: (Fig. 1)

删除了: soil organic carbon

删除了: M

删除了: (

删除了: β-1

删除了:)

删除了: , Tse three enzymes were selected because theythe

设置了格式: 非突出显示

删除了: ref??

设置了格式: 非突出显示

删除了: decomposition

删除了: more

decomposition. Given that enzymes have a low carbon content and their inclusion a pool could lead to model overparameterization, we therefore assign them a catalysis role instead of considering them as carbon pools. In these three model schemes, SM1 and SM2 implicitly represent microbial activities, where the decomposition of SOM governed by linear, first- order dynamics. Soil C turnover times are defined by biome and pool-specific decay constants, which are modified by environmental scalars such as soil temperature and soil moisture availability (Du et al., 2017; Du et al., 2025). In contrast, the SM3 adopted reverse Michaelis-Menten kinetics to explicitly represent the catalytic progress of microbial extracellular enzymes. The turnovers of DOC, POC and MAOC are depended on the size of both the donor (substrate) and the receiver (microbial biomass) pools. SM1 was expressed by the following equations:

$$\frac{dC_M}{dt} = I + C_S c_7 a_{67} + C_P c_8 a_{68} - C_M c_6 \quad (1)$$

$$\frac{dC_S}{dt} = I + C_M c_6 a_{76} - C_S c_7 \quad (2)$$

$$\frac{dC_P}{dt} = C_M c_6 a_{86} + C_S c_7 a_{87} - C_P c_8 \quad (3)$$

Where C_M, C_S, C_P represent the C content of microbe, slow SOM and passive SOM. I represents the C input from litters, c_6, c_7, c_8 represent the exit rate of C from microbes, slow SOM and passive SOM, and a_{67}, a_{68}, a_{76}, a_{78} represent the allocation of slow SOM to microbes, passive SOM to microbes, microbes to slow SOM and passive SOM to slow SOM, respectively.

The soil C pools of SM2 were expressed as follows:

$$\frac{dC_{DOC}}{dt} = I + C_{POC} c_7 a_{67} + C_{MAOC} c_9 a_{69} - C_{DOC} c_6 \quad (4)$$

删除了: pools

删除了: which directly catalyze the decomposition of POC and MAOC.

删除了:

删除了:

删除了: 6

带格式的: 缩进: 首行缩进: 0 厘米

删除了:

删除了:

带格式的: 缩进: 首行缩进: 1.18 字符

$$\frac{dC_{POC}}{dt} = I + C_M c_8 a_{78} - C_{POC} c_7 \quad (5)$$

$$\frac{dC_M}{dt} = C_{DOC} c_6 a_{86} - C_M c_8 \quad (6)$$

$$\frac{dC_{MAOC}}{dt} = C_{POC} c_7 a_{97} + C_M c_8 a_{98} - C_{MAOC} c_9 \quad (7)$$

Where C_{DOC}, C_{POC}, C_{MAOC} represent the C content of DOC, POC, MAOC. Parameters c_6, c_7, c_8, c_9 denote the exit rate of DOC, POC, microbes and MAOC, and a_{67}, a_{69}, a_{78}, a_{86}, a_{97}, a_{98} represent the allocation of POC to DOC, MAOC to DOC, microbes to POC, DOC to microbes, POC to MAOC and microbes to MAOC, respectively. SM3 was expressed by the following equations:

$$\frac{dC_{DOC}}{dt} = I + a_{67}(V_{CBH.P} + V_{PPO.P} + V_{BG.P})C_{POC} + a_{69}(V_{CBH.M} + V_{PPO.M} + V_{BG.M})C_{MAOC} - \frac{V_{max.assim} C_M C_{DOC}}{KM_{assim} + C_{DOC}} \quad (8)$$

$$\frac{dC_{POC}}{dt} = I + C_M c_8 a_{78} - (V_{CBH.P} + V_{PPO.P} + V_{BG.P})C_{POC} \quad (9)$$

$$\frac{dC_M}{dt} = C_{DOC} c_6 a_{86} - C_M c_8 \quad (10)$$

$$\frac{dC_{MAOC}}{dt} = a_{97}(V_{CBH.P} + V_{PPO.P} + V_{BG.P})C_{POC} + a_{98} c_8 C_M - (V_{CBH.M} + V_{PPO.M} + V_{BG.M})C_{MAOC} \quad (11)$$

Where $V_{max.assim}$ and KM_{assim} denote microbe maximum assimilation rate and half-saturation for assimilation. $V_{CBH.P}$, $V_{PPO.P}$, $V_{BG.P}$ represent catalytic rate of CBH, PPO, BG to POC. $V_{CBH.M}$, $V_{PPO.M}$, $V_{BG.M}$ represent catalytic rate of CBH, PPO, BG to MAOC.

$$V_{enzy.P} = \frac{V_{max.enzy} f_{enzy} C_M}{KM_{enzy} + C_{POC}} \quad (12)$$

$$V_{enzy.M} = \frac{V_{max.enzy} f_{enzy} C_M}{KM_{enzy} + C_{MAOC}} \quad (13)$$

删除了:

删除了:

删除了:

Where $V_{max.enzy}$ represent the maximum reaction rate. KM_{enzy} represent half-saturation for reaction, f_{enzy} represent the C ratio of CBH, PPO, BG to microbes, respectively. The enzyme activities were calculated as following:

$$V_{enzy} = \frac{V_{max.enzy} f_{enzy} C_M C_{sub}}{KM_{enzy} + C_{sub}} \quad (14)$$

Where C_{sub} denotes the C content of the enzyme-catalyzed substrate contained within a soil block with an area of 1 m^2 and a depth of 10 cm, and it maintains a consistent ratio of enzyme to substrate as required for experimental measurements.

To quantify model uncertainty, we employed the MCMC data assimilation method (Xu et al., 2006) to invert model parameters (Table A1). Subsequently, 1,000 sets of parameters were randomly sampled from the posterior distribution of each parameter to generate predictions (Fig. 3). The standard deviation of the 1,000 simulation results for total organic carbon (TOC) in the year 2100 from each model was used to represent the magnitude of uncertainty arising from model parameters. The traceability analysis framework (Supplement) was used to evaluate changes in the simulated ecosystem C storage capacity. The effect of drought on C storage is calculated as follows:

$$Drought\ Effect = \frac{(C_{drought} - C_{ctr})}{C_{ctr}} \times 100\% \quad (15)$$

Where $C_{drought}$ represents the C content of drought, C_{ctr} represents the C content of control condition.

3 Results

3.1 Model validation

删除了:

删除了:

删除了:

带格式的: 缩进: 首行缩进: 0.74 厘米

删除了: We estimated model parameters using the Markov Chain Monte Carlo (MCMC) and evaluated changes in the simulated ecosystem C storage capacity using a traceability analysis framework (Supplement).

删除了:

删除了:

In this study, we used the Markov Chain Monte Carlo (MCMC) algorithm to constrain model parameters (Figs. 2 and A3). All schemes incorporate 8 vegetation-related parameters (Fig. A3). SM1 included 8 soil carbon-related parameters (Fig. 2), with 5 well-constrained under control conditions (c_7, a_{86}, a_{67}, a_{87}, a_{68}) and 5 under drought conditions (c_7, c_8, a_{76}, a_{86}, a_{68}). SM2 consisted 14 soil carbon-related parameters, with 7 well-constrained in the control scenario (c_9, c_{10}, a_{74}, a_{65}, a_{67}, a_{97}, a_{78}) and 9 in the drought scenario (c_9, c_{10}, a_{64}, a_{74}, a_{86}, a_{67}, a_{97}, a_{98}, a_{69}). SM3 had 11 well-constrained parameters under control conditions ($V_{max.assim}$, $V_{max.CBH}$, KM_{CBH}, f_{CBH}, f_{BG}, f_{PPO}, a_{64}, a_{74}, a_{75}, a_{97}, a_{78}) and 12 under drought conditions (c_6, $V_{max.assim}$, $V_{max.CBH}$, KM_{CBH}, KM_{BG}, $V_{max.PPO}$, KM_{PPO}, f_{BG}, f_{PPO}, a_{65}, a_{86}, a_{97}) in all 22 soil carbon-related parameters.

All three schemes calibrated by observations from the drought experimental which had overall good agreement (Figs. A1 and A2). The simulation of vegetation C (leaf, fine root, wood) and soil respiration exhibited high accuracy. The simulated MBC by SM1 was inferior to those simulated by SM2 and SM3, suggesting that incorporating measurable C pools can improve the accuracy of MBC simulation. By comparing the accuracy of POC and MAOC, we found that SM3 generally outperformed SM2, indicating that the incorporation of enzyme activities can enhance the simulation of the SOC fractions, particularly with respect to MAOC.

3.2 Carbon simulation and prediction by three model schemes

Carbon storage from 2023 to 2100 was predicted using three different model schemes. All models consistently indicated an increasing trend in vegetation C (VegC) and a decreasing trend in SOC under both control and drought conditions (Figs. 3 and A4).

删除了: S
删除了: three
删除了: S
删除了: S
删除了: S
删除了: soil organic carbon
删除了: S

Specifically, under control conditions, SM1 simulated change rates of 260% for VegC, -56.9% for SOC and 188% for total organic carbon (TOC). Under drought conditions, the corresponding rates were 223%, -50.4% and 159%. SM2 projected growth rates of 263% for VegC, -60.8% for SOC and 179% for TOC under control conditions, and 217%, -55% and 151% under drought. For SM3, the simulated growth rates were 230% for VegC, -88% for SOC and 146% for TOC in the control scenario, while under drought the values were 169%, -55% and 106%, respectively.

The coefficient of variation (CV) of predicted TOC in 2100 across 1,000 parameter sets was 0.12 for SM1, 0.15 for SM2, and 0.22 for SM3. Importantly, the difference between the highest and lowest median TOC predictions among the three models (SM1, 5.2, SM2, 4.1, SM3, 3.8 kg C m^{-2}) is approximately 2.5 times larger than the average within-model parametric uncertainty (mean SD, 0.6 kg C m^{-2}), demonstrating that model structural uncertainty dominates (Fig. 3j).

3.3 Drought effects on carbon storage

All three modeling schemes consistently indicated that drought reduced C content in MBC (SM1, -36.9%; SM2, -56.9%; SM3, -27.3%), VegC (SM1, -16.8%; SM2, -19.9%; SM3, -25.4%) and TOC (SM1, -15%; SM2, -19.4%; SM3, -24.4%). However, the simulated responses of SOC to drought varied among the schemes (Fig. 4). SM1 predicted an increase in SOC under drought conditions (+39.5%) compared to the control, driving by increases in both the slow (+13%) and passive (+57%) C pools. Similarly, SM3 projected a rise in SOC (+56.9%), accompanied by increases in POC (+82.3%), MAOC (+88.1%), and DOC (+6.7%). In contrast, SM2 simulated a decrease

删除了: growth

带格式的: 缩进: 首行缩进: 1.18 字符

删除了: $^{-2}$

设置了格式: 上标

删除了: $^{-2}$

删除了: The uncertainty analysis shows that the median TOC simulated by SM3 differs significantly from that of SM1 and SM2, indicating that SM3 introduces greater uncertainty due to its model structure

删除了: 4

in SOC (-6.1%), with reductions in DOC (-35.3%) and MAOC (-3.7%), through POC increased (+43.4%).

By comparing the proportion of drought effects on each carbon pool simulated by each model to the total drought effects across the three models, it is apparent that different modeling schemes exhibit distinct sensitivities to drought (Fig. 4). Specifically, SM2 demonstrated greater sensitivity to drought effects on microbial biomass (-54%) and DOC (-84%) compared to SM3 (-18% and +16%, respectively). Conversely, SM3 showed higher sensitivity to drought-induced changes on POC (+82%) and MAOC (+74%) relative to SM2 (-26% and +18%, respectively).

3.4 Traceability analysis of drought effects

The traceability analysis revealed that both SM1 and SM3 simulated higher SOC under drought condition (SM1, 2.5 kg C m^{-2}; SM3, 1.2 kg C m^{-2}) compared to the control (SM1, 2.1 kg C m^{-2}; SM3, 0.8 kg C m^{-2}) at the end of forecast period (Fig. 5). In contrast, SM2 simulated lower SOC under drought (2.3 kg C m^{-2}) compared to the control (2.5 kg C m^{-2}). The increase of SOC in SM1 during drought was driven by higher soil carbon input (drought, 1.0 kg C m^{-2} $year^{-1}$; control, 0.6 kg C m^{-2} $year^{-1}$) (Figs. 4), while in SM3, it resulted from an extended soil carbon residence time (drought, 4.3 years; control, 2.6 years). However, SM2 simulated a reduction in soil carbon residence time under drought, leading to decreased SOC.

We further analyzed the C residence times of individual pools simulated by the three modeling schemes under both control and drought conditions (Fig. 4c). In SM1, drought increased the C residence time of passive SOM. For SM2, drought reduced the C

删除了: By comparing the proportion of drought effects on each soil C pool simulated by each scheme

删除了: across specific carbon pools

删除了: 4

删除了: 5 and 6

删除了: 6

删除了: which resulted from the allocation proportions from slow SOM to passive SOM and from passive SOM to microbes were elevated

residence time of microbes and increased that of MAOC. In SM3, drought resulted in a longer C residence time for MAOC.

4 Discussion

4.1 Response of ecosystem carbon dynamics to long-term drought

In this study, all three modeling schemes consistently indicate that drought leads to decrease in vegetation carbon, microbes carbon (Microbe C) and total organic carbon (TOC), while POC increases under drought conditions (Figs. 3, 4 and A4). These findings are consistent with multiple fields manipulated experiments (Zhou et al., 2020; Pennisi, 2022; Schwalm et al., 2017). During drought, plants undergo physiologically adjustments and shifts in community structure in accordance with species-specific water use strategies to prevent excessive water loss (Rowland et al., 2023). These responses in turn affect C uptake via photosynthesis and C release via respiration at the ecosystem level, potentially decoupling these two processes (Meir et al., 2008).

Drought consistently reduced microbial biomass carbon (MBC) across all three models, and sensitivity analysis indicated this reduction was primarily driven by increased microbial decay rates (Figs. 2 and A5). With prolonged drought duration, microbial C content exhibited a pattern of initial decline followed by a gradual recovery (Fig. 3b). Drought-induced water stress directly impairs microorganisms, leading to decreased metabolic activity (Quiroga et al., 2024). However, microorganisms can adapt to drought through physiological changes, community turnover, and evolutionary mechanisms (Martiny et al., 2015; Allison, 2023). At the community scale, drought-sensitive microbes may be replaced by more resilient taxa that immigrate into the area

删除了: . The allocation proportions from POC to DOC and from DOC to microbes were enhanced, while the allocation from MAOC to DOC declined

删除了: The allocation proportions from DOC to microbes, from MAOC to DOC, and from microbes to MAOC all increased, while the allocation from microbes to POC decreased.

删除了:

删除了: vegetable carbon (

删除了: V

删除了: C

删除了:)

删除了: particulate organic carbon (

删除了:)

删除了: S

删除了: .

删除了: S

删除了: a

删除了: .

(Allison et al., 2008; Ricks & Yannarell., 2023). Several studies have showed that fungi exhibit greater drought adaptability compared to bacteria (Preece et al., 2019; Bastida et al., 2018; Williams & de Vries et al., 2018). Gram-positive bacteria are also better adapted to low-moisture soils compared to Gram-negative bacteria, due to their thicker and harder cell walls, which render them less affected by drought (Castro et al., 2010). Through in situ manipulation experiments at the same site, Bu et al (2018) and Su et al (2020b) have observed that drought slightly reduced MBC and microbial biomass nitrogen (MBN), and significantly altered the microbial community structure. Drought significantly increased the relative abundance of Acidobacteria, which was primarily associated with the decrease in soil pH, while the relative abundance of Proteobacteria decreased significantly. Besides, the red-yellow soil at the Tiantong site is rich in Fe/Al oxyhydroxides (e.g., hematite, goethite) and kaolinite, which provide a high specific surface area and strong adsorption capacity for microbial necromass and DOC (Wang et al., 2025). Given that microbes directly consume DOC, the incorporation of measured DOC pools in SM2 and SM3 enhances the model's ability to simulate microbial sensitivity to drought (Fig. 4b).

Simulation results from all three modeling schemes consistently showed that drought initially decreased soil respiration, followed by a subsequently recovery (Fig. 3a). This trend mirrors variations in microbial carbon content, indicating that drought regulates soil respiration primarily through its control of microbial biomass (Zhao et al., 2025; Ficken & Warren., 2019). All three schemes consistently simulated an increase in particulate organic carbon (POC) under drought (Fig. 4b). This cross-model

设置了格式: 非突出显示

删除了: ; Uhlírová et al., 2005

删除了: and Su et al (2020b) have observed shifts in microbial community structure under drought condition, which may explain the gradual increase in microbial biomass under prolonged drought conditions.

删除了: g

consistency arises from multiple ecological mechanisms that are represented, albeit differently, across the three model structures (Du et al., 2015; 2017).

First, drought causes plants to allocate more carbon belowground to acquire water, resulting in the increase in root-to-shoot ratio, root dry weight and root morphological characteristics (Ulrich et al., 2022; Williams et al., 2020; Reinelt et al., 2023). Tracing analysis shows that soil carbon input simulated by the three models increased under drought conditions (Fig. 5d). In situ manipulation experiments found that the specific root length, specific surface area, and fine root biomass of the four dominant local plant species (e.g., *Castanopsis sclerophylla, Schima superba, Castanopsis carlesii, Lithocarpus glaber*) all increased significantly under drought stress (Jiang et al., 2023). This root-derived carbon input is a direct source of POC, as coarse root litter and particulate root fragments are physically classified as POC. In SM1, this increased input enters the slow SOM pool, which functionally overlaps with POC in terms of turnover time and substrate quality (Fig. 5). In SM2 and SM3, these inputs are explicitly routed to the POC pool via litter transfer coefficients (a_{74}, a_{75}).

Second, drought suppresses microbial decomposition activity (Feng et al., 2025). Reduced soil moisture limits extracellular enzyme diffusion, lowers microbial metabolic efficiency, and decreases the activities of POC-degrading enzymes such as cellobiohydrolase and β-glucosidase (Su et al., 2020b; Wu et al., 2025). This suppression is represented in SM1 and SM2 indirectly through soil moisture scalar functions that reduce decomposition rates of all pools, whereas SM3 explicitly captures

删除了:

设置了格式: 字体: 非倾斜

删除了:

the reduction via enzyme kinetic parameters (*Vmax*, *KM*) and enzyme-to-microbial carbon ratios (f_{CBH}, f_{BG}, f_{PPO}).

Third, drought-induced changes in soil physicochemical properties suppress the decomposition of SOC. Drought-induced soil aggregate dynamics may physically protect POC from decomposition. Although not explicitly modeled in any of the three schemes, the net effect of reduced POC loss relative to input is emergent in all three model structures. The correlation between soil physicochemical properties and soil carbon mineralization rates indicates that soil moisture content, total carbon (TC), total phosphorus (TP), inorganic nitrogen (IN), available phosphorus (available-P), TC/TP, TN/TP, and IN/available-P are key factors. Soil carbon mineralization rates are positively correlated with soil moisture content, TC/TP, TN/TP, and IN/available-P. Drought led to a decrease in these physicochemical properties. In contrast, soil carbon mineralization rates are negatively correlated with available-P, which increases under drought conditions (Su et al., 2020a).

4.2 Divergent simulations of drought effect on SOC among three modeling schemes

A key divergence among the three modeling schemes lies in their simulation of drought effects on SOC components, which is the key source of discrepancy in the projected carbon storage response (Figs. 4). SM1 divides SOC into three pools, including MBC, slow SOM, and passive SOM. However, since only total SOC data are available to constrain the model, the predictions of this scheme are highly sensitive to the quality and the duration of SOC observations. Given the non-linear response of ecosystems to

设置了格式: 字体: 倾斜

设置了格式: 字体: 倾斜

设置了格式: 字体: 倾斜

删除了: Therefore, the consistent POC increase across models reflects that drought enhances POC inputs through root allocation shifts while simultaneously suppressing POC decomposition by limiting microbial activities and altering soil physicochemical properties. The magnitude of increase varies among models (SM3 > SM2 > SM1), with SM3 showing the largest response due to its explicit representation of enzyme-mediated decomposition and its sensitivity to moisture-induced enzymatic suppression.

删除了: Sensitive analysis further revealed a strong positive correlation between the C content of POC and the allocation proportion of litters to POC (Figs. 2 and S5). These results imply that drought enhance both the carbon content in litter and its transfer to POC, resulting in an overall increase in POC. Furthermore, since POC are directly influenced by enzymatic catalysis, SM3's heightened sensitivity to drought effects on these pools underscores the model's effectiveness in capturing enzyme-mediated processes under drought conditions.

删除了: and 6

删除了: (Fig. S5)

drought duration (Müller et al., 2022; Anderegg et al., 2020; Schwalm et al., 2017), models constrained by short-term observation data may introduce substantial deviation in long-term projections. In contrast, SM2 partitions the SOC into four observable carbon pools (i.e., Microbes, POC, MAOC and DOC), each independently constrained by corresponding measurements. The trajectory of SOC is thus jointly determined by these four fractions, leading to pronounced differences between the predictions of SM1 and SM2. Given that both models use the same SOC data, this highlights the profound influence of carbon partitioning strategies on model predictions. Furthermore, drought causes the carbon input rates and carbon loss rates of individual carbon pools in SM2 deviate from the overall SOC change rate. These pool-specific discrepancies cause the SOC predictions to diverge increasingly over time between models with different structures.

The differences between SM2 and SM3 are mainly reflected in the dynamics of DOC and MAOC. SM2 employs first-order linear kinetics to describe the decomposition of DOC and MAOC, where the decomposition rate is proportional to their C content. In contrast, SM3 uses reverse Michaelis-Menten kinetics, meaning that SOC decomposition depends not only on substrate carbon content but also on microbial biomass and enzyme activities (Chandel et al., 2023). Under drought, SM2 simulates a decrease in DOC, while SM3 predicts an increase (Fig. 4). Some studies report that drought reduces DOC concentrations (Tiwari et al., 2022; Wu et al., 2023), whereas others suggest it may increase DOC due to factors such as air temperature, soil temperature, humidity, precipitation, pH, and sulfate concentrations (Evans et al., 2005;

删除了: Since both models use the same SOC data, this demonstrates the profound influence of carbon partitioning strategies on model predictions.

删除了: Despite the divergent SOC responses among models, all three schemes consistently simulated an increase in particulate organic carbon (POC) under drought (Fig. 4b). This cross-model consistency arises from multiple ecological mechanisms that are represented, albeit differently, across the three model structures (Du et al., 2015; 2017). First, drought induces a shift in plant carbon allocation belowground, such as increase fine root biomass, specific root length, and rhizodeposition (Jiang et al., 2023). This root-derived carbon input is a direct source of POC, as coarse root litter and particulate root fragments are physically classified as POC. In SM1, this increased input enters the slow SOM pool, which functionally overlaps with POC in terms of turnover time and substrate quality (Fig ??). In SM2 and SM3, these inputs are explicitly routed to the POC pool via litter transfer coefficients (a_{67}, a_{78}). Second, drought suppresses microbial decomposition activity (ref??). Reduced soil moisture limits extracellular enzyme diffusion, lowers microbial metabolic efficiency, and decreases the activities of POC-degrading enzymes such as cellobiohydrolase and β-glucosidase (Su et al., 2020b; Wu et al., 2025). This suppression is represented in SM1 and SM2 indirectly through soil moisture scalar functions that reduce decomposition rates of all pools, whereas SM3 explicitly captures the reduction via enzyme kinetic parameters (*Vmax*, *KM*) and enzyme-to-microbial carbon ratios (f~CBH~*, *f~BG~*, *f~PPO~*). Third, ...

删除了: Differences

删除了: utilizes

删除了: indicates

删除了: the

删除了: of SOC is not only

删除了: ent

删除了: C

删除了: C

删除了: condition

删除了: can

删除了: the influence of

Sowerby et al., 2010). Sensitivity analysis reveals that DOC in SM2 is influenced mainly by the transfer ratios of POC to DOC and metabolic litter to DOC (Fig. A5). However, in SM3, DOC dynamics are primarily controlled by the microbe maximum assimilation rate and half-saturation for assimilation, indicating that SM3 captures direct microbial regulation of DOC decomposition. Similarly, while SM2 simulates a slight decrease in MAOC under drought, SM3 predicts an increase (Fig. 4). This discrepancy stems the fact that SM3 explicitly incorporates the catalytic effects of three enzyme activities (BG, PPO and CBH) on MAOC decomposition. Long-term drought at this site drives a shift toward fungal-dominated microbial communities (Bu et al., 2018; Su et al., 2020b). Fungi are major producers of oxidative and hydrolytic enzymes (PPO, CBH, BG). SM3 explicitly represents these enzymes, thereby capturing drought-induced declines in catalytic rates and MAOC accumulation—a key mechanism absent in SM2's implicit microbial representation. This explains why SM3 outperforms SM2 in simulating POC and MAOC dynamics (Fig. A2) and highlights the importance of integrating microbial physiology and site-specific mineralogical and ecological traits into SOC models.

4.3 Implications for future research and model development

Our study enhances the understanding how drought affects forest C dynamic across different model schemes. Nevertheless, we acknowledge that several uncertainties involved in our analysis. First, we only considered three enzymes that directly catalyze soil carbon decomposition. Other enzymes (e.g., Acid phosphatase, N-acetyl-glycosaminidase, Peroxidase) may also contribute indirectly to this process (Su et al., 2020b), but they were not included because their primary roles are in nutrient cycling.

删除了: the transfer ratio of

删除了: S

删除了: in SM3

删除了: -

删除了: –

设置了格式: 字体: 倾斜

下移了 [1]: (Bach et al., 2016; Waldrop et al., 2006)

移动了(插入) [1]

删除了: These three enzymes provide a parsimonious yet functionally representative set for capturing drought effects on SOC decomposition. Other enzymes (e.g., acid phosphatase, N-acetyl-glucosaminidase, peroxidase) were excluded because they are primarily involved in nutrient acquisition (nitrogen, phosphorus) or exhibit functional redundancy with the selected enzymes for carbon depolymerization, and their inclusion would increase model complexity without proportional improvement in predictive accuracy for carbon dynamics, particularly given the limited availability of observational constraints (Du et al., 2015; ref??). Drought reduces microbial enzyme activities (Figs. S1 and S2) (Bach et al., 2016; Waldrop et al., 2006), thereby weakening MAOC decomposition capacity and accumulating allowing MAOC to accumulate under drought conditions (Bach et al., 2016; Waldrop et al., 2006). Moreover, the explicit inclusion of enzyme-mediated processes significantly improves the accuracy of POC and MAOC simulations (Fig. A2), suggesting highlighting the importance of representing enzyme activities in SOC decomposition models.
The divergent drought effects among models are further explained by site-specific ecological characteristics. The red-yellow soil at the Tiantong site is rich in Fe/Al ...

设置了格式: 字体: 加粗

带格式的: 缩进: 首行缩进: 0 字符

删除了: ,

删除了: while o

删除了: .

删除了: which

删除了: excluded

删除了: y are primarily involved

删除了: acquisition

Including them would substantially increase model complexity and parameter identifiability issues, especially given the lack of direct constraints from available enzyme activity data. Second, when calculating enzyme activities, we applied laboratory-derived proportional relationships between enzyme quantity and substrate quantity to field conditions, which assumes substrate availability far exceeds enzyme availability in field soils. Finally, laboratory enzyme activity measurements typically use specific substrates, whereas field soils contain multiple potential substrates that could be catalyzed, which introduces additional uncertainty in our simulations.

Although our results demonstrate that incorporating measurable carbon pools or increasing model complexity can improve simulation accuracy for specific carbon fractions and capture nonlinear drought responses, this does not imply that all land surface models should adopt the SM2 or SM3. The appropriate model selection depend on research objectives, data availability, and computational constraints. Specifically, SM1 remains sufficient for large-scale simulations and long-term carbon budget assessments. SM2 is preferable when the goal is to investigate the dynamics of carbon fractions (e.g., POC, MAOC, DOC) and their compositional changes. SM3 becomes essential for exploring nonlinear ecosystem responses to extreme climate events such as drought, warming, or other perturbations. Particularly, the advantages of SM2 and SM3 are contingent upon the availability of observational data for model calibration. Without sufficient constraints, increased complexity can lead to greater parameter uncertainty and reduced robustness. Therefore, future model development should

删除了: (nitrogen, phosphorus) or exhibit functional redundancy with the selected enzymes for carbon depolymerization. Besides, i

删除了: a larger number of enzymes

删除了: dimensionality, potentially leading to parameter non-identifiability and increased uncertainty, especially given the limited availability of observational constraints. Therefore, the current model adopts a parsimonious representation aimed at balancing process realism and parameter tractability

删除了: ies

设置了格式: 非突出显示

删除了: show

带格式的: 缩进: 首行缩进: 0.42 厘米

删除了: using observable carbon pools or increasing model complexity

删除了: the

删除了: pools

删除了: the

删除了: to drought,

删除了: should

删除了: the

删除了: costs

删除了: If the objective is large-scale simulation and long-term carbon budget prediction, SM1 likely suffices. For investigating carbon pools dynamics and components change, SM2 is preferable. To explore nonlinear responses to drought, warming, or extreme climate events, SM3 is essential

删除了: In p

删除了: rely on

删除了: such data

删除了: may

删除了: higher

pursue a balanced strategy, introducing additional process representations only when they are supported by data and justified by the specific application.

5 Conclusions

Accurately simulating drought impacts on soil carbon dynamics is critical for predicting terrestrial carbon sequestration. In this study, we integrated data assimilation and traceability analysis to evaluate three soil carbon decomposition schemes, examining how different model structures simulate soil carbon responses to drought. Our results revealed significant disparities in drought effects on soil organic carbon (SOC) among the three models, with these differences primarily driven by variations in carbon input and carbon residence times across pools. Explicitly incorporating microbial enzyme activities notably altered the impacts of drought on mineral-associated organic carbon and dissolved organic carbon. These findings underscore the critical roles of carbon pool partitioning schemes, their empirical constrainability, and the consideration of microbial enzyme catalytic processes in simulating SOC response to drought, thereby advancing our understanding of the complex mechanism governing drought-induced soil organic carbon dynamics.

删除了: aim for
删除了: where additional process representations are
删除了: ed
删除了: only when supported by data and justified by the targeted application
删除了:
删除了: the
删除了: of drought
删除了: of
删除了: importance
删除了: , devising three soil carbon decomposition schemes and exploring how different soil carbon decomposition models simulate soil carbon responses to drought
删除了: the
删除了: as simulated by
删除了: of different carbon
删除了: significant
删除了: different
删除了: the
删除了: of soil carbon
删除了: enhancing
删除了: ity
删除了: underlying
删除了: effects on
删除了: decomposition

Acknowledgments: This research was financially supported by the National Natural Science Foundation of China (Grant No. 32241032, 31930072, 32471683, 32071593) and the Fundamental Research Funds for the Central Universities (Grant No. 2572022BA08); Heilongjiang Touyan Innovation Team Program (Forest Carbon Sink Assessment and Carbon Sequestration Management Innovation Team).

CRediT author contribution statement: F.D and Z.D. collected and analyzed the data and wrote the manuscript. Z.D. conceived, designed, and oversaw the study. F.D., L.F., and Z.G. conducted the statistical analysis. F.D., X.Z., and Z.D. discussed, wrote, and revised the manuscript with major contributions from L.Z. Y.Z. and G.Z. commented on the manuscript.

Competing interest declaration: Authors declare that they have no competing interests.

Data and materials availability: Data will be made available on request.

删除了:

删除了: OMPETING INTEREST DECLARATION

删除了: ATA

删除了: AND

删除了: MATERIALS

删除了: AVAILABILITY

设置了格式: 非突出显示

设置了格式: 非突出显示

设置了格式: 非突出显示

设置了格式: 非突出显示

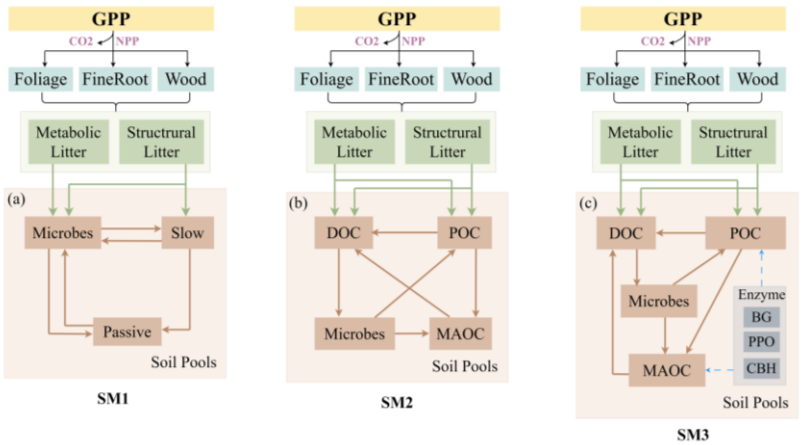

888

889 **Figure 1.** Conceptual diagram of the soil biogeochemical models with three schemes.
890 **(a)** conventional three-pool partitioning scheme (SM1), **(b)** mineral and particulate-
891 associated carbon partitioning scheme (SM2), and **(c)** Michaelis-Menten regulated
892 carbon-stabilization scheme (SM3). All pools (boxes) and fluxes (arrows) represent C
893 process. BG, β-1, 4-glucosidase, PPO, polyphenol oxidase, CBH, cellobiohydrolase.
894

删除了:

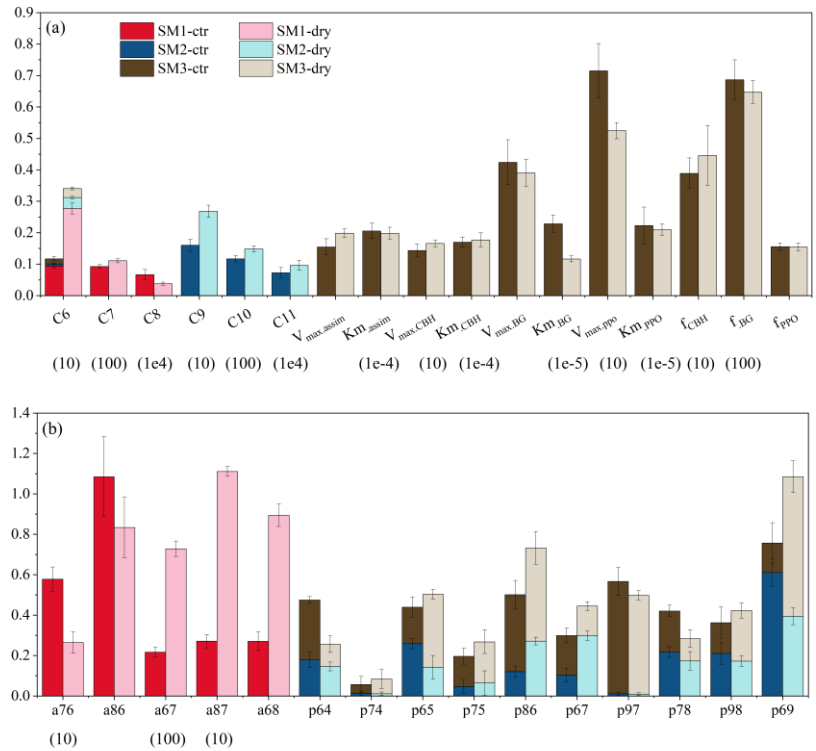

Figure 2. Maximum likelihood estimates (MLEs; or means for unconstrained parameters) of the target parameters under control and drought treatments across the three schemes. Error bars indicate standard deviations (SDs). Refer to Table A1 for parameter abbreviations and units.

删除了: value
删除了:) (
删除了: in both
删除了: among
删除了: represent
删除了: See
删除了: S

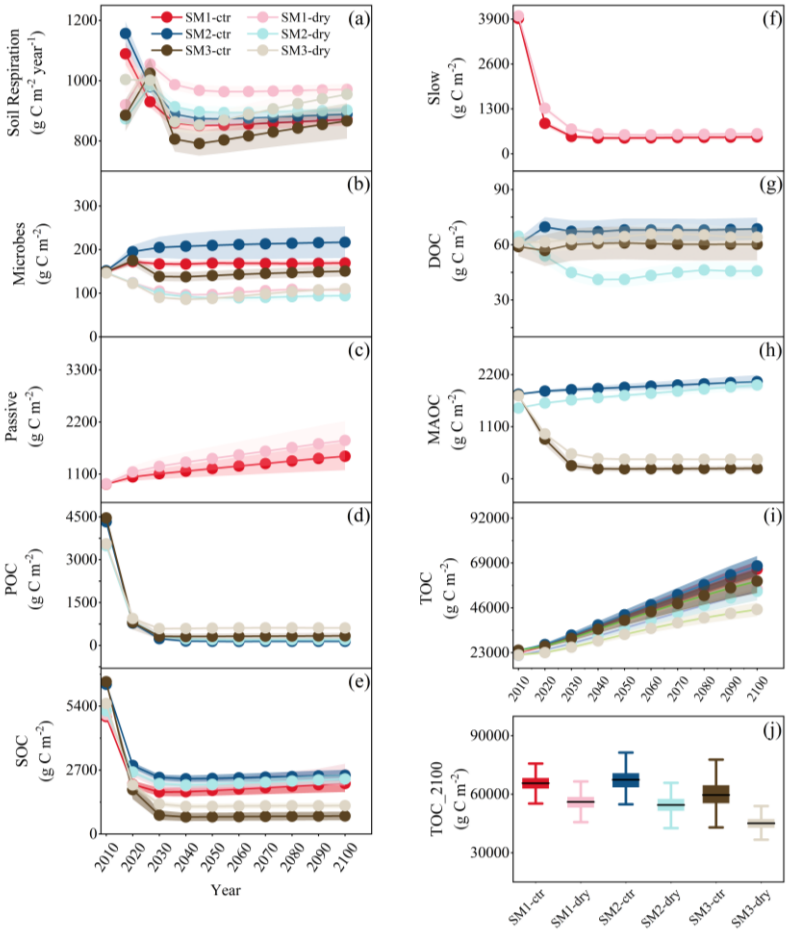

912

913 **Figure 3.** Predicted soil respiration **(a)**, microbial C **(b)**, passive SOM **(c)**, POC **(d)**,
914 SOC **(e)**, slow SOM **(f)**, DOC **(g)**, MAOC **(h)**, total organic C **(i)** from 2014 – 2100
915 under dry and control conditions for the three schemes, and (j) the mean TOC in 2100
916 predicted by 1000 simulations.
917

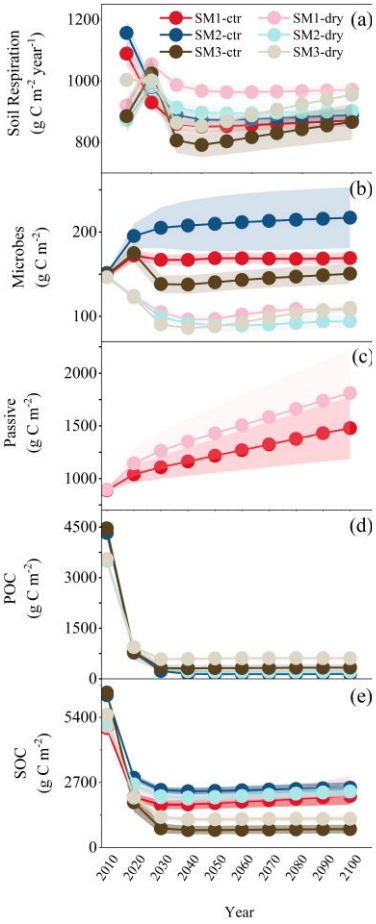

删除了:

删除了: .

删除了: represents

设置了格式: 非突出显示

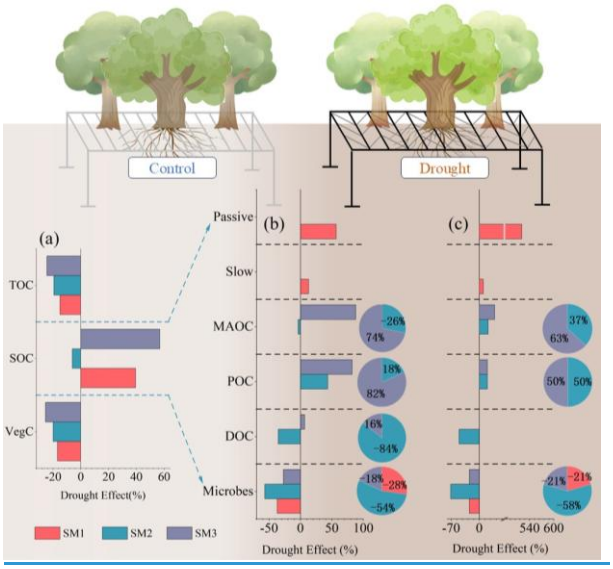

Figure 4. Conceptual diagram illustrating the effects of drought simulated by the three schemes on carbon stocks. (a) Drought effects on soil total organic carbon (TOC), soil organic carbon (SOC), and vegetation carbon (VegC) in 2100. (b) Drought effects on individual carbon pools; pie charts indicate the proportional contribution of each scheme to the total drought effect on each pool. (c) Drought effects on carbon residence time across pools; pie charts represent the proportional contribution of each scheme to the total drought effect on the carbon residence time of each pool.

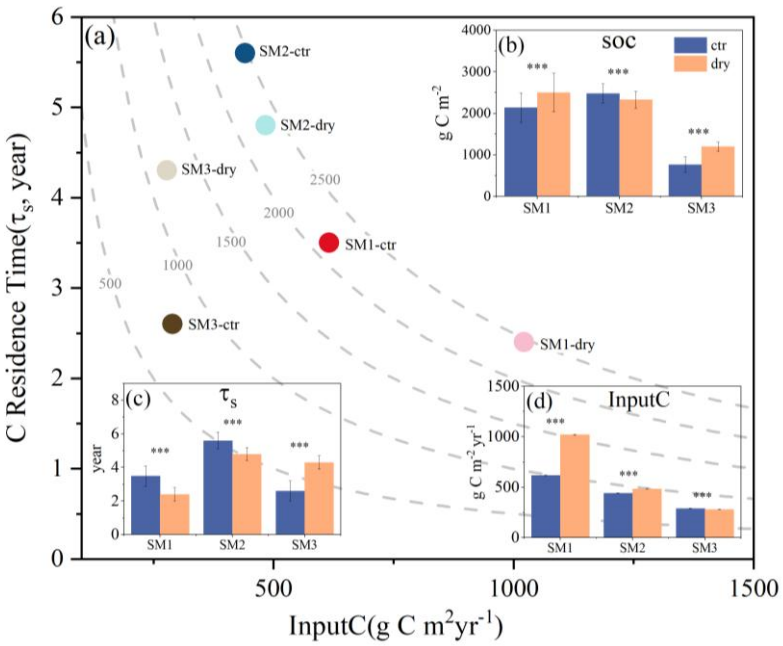

Figure 5. Predicted soil C storage capacity in 2100 by C influx (InputC, x axis) and soil carbon residence time (τ_s, y axis) between control and drought treatments in three model schemes. ***, represents $p < 0.01$.

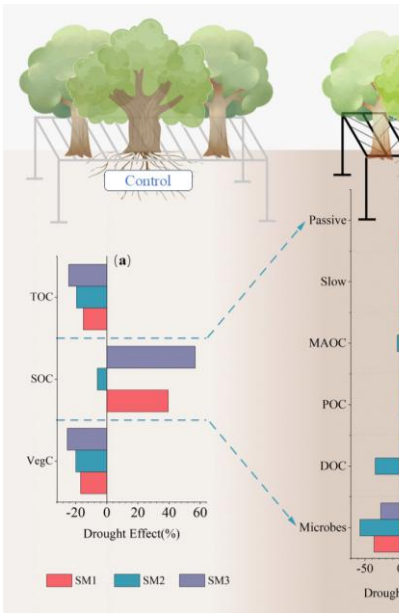

删除了:

Figure 4. Conceptual figure of the effects of drought simulated by three schemes on carbon stocks. The histogram represents the drought effects on carbon pools (percentage change of the carbon pools from 2022 to 2100), and corresponding pie charts represent the proportion of the drought effects simulated by each of the three schemes for the same carbon pool, relative to the sum of the drought effects from all three schemes. TOC, soil total organic carbon. VegC, vegetation carbon.

分页符

删除了: 5

Appendix

删除了:

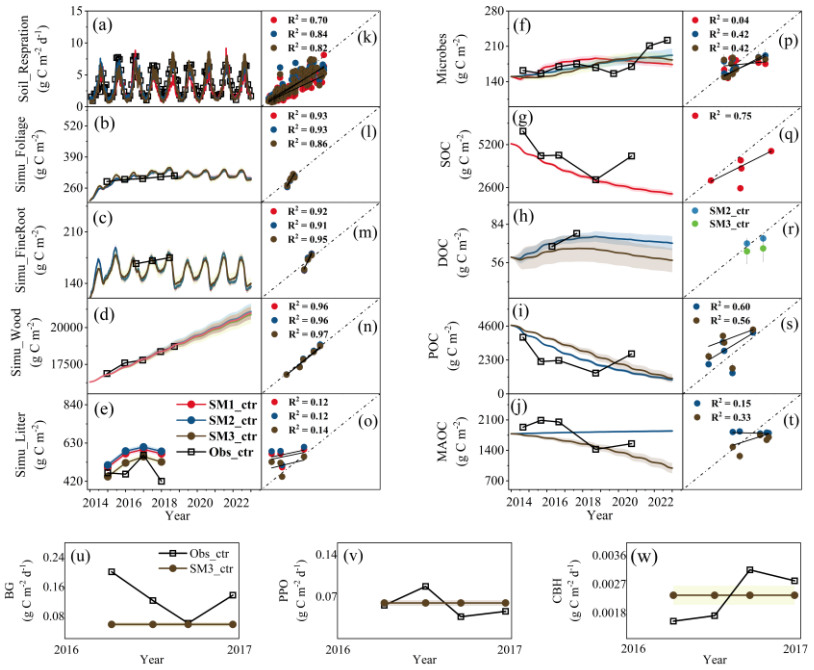

Figure A1. Comparison of the measured values (black squares) and simulated values (lines) in the control conditions of three schemes from 2014 to 2022, $p < 0.05$.

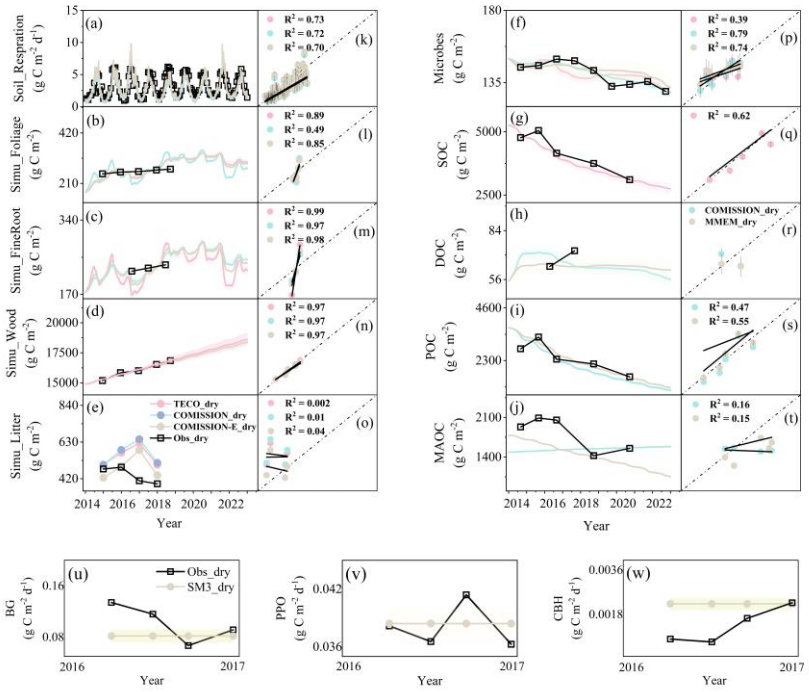

Figure A2. Comparison of the measured values (black squares) and simulated values (lines) in the drought conditions of three schemes from 2014 to 2022, $p < 0.05$.

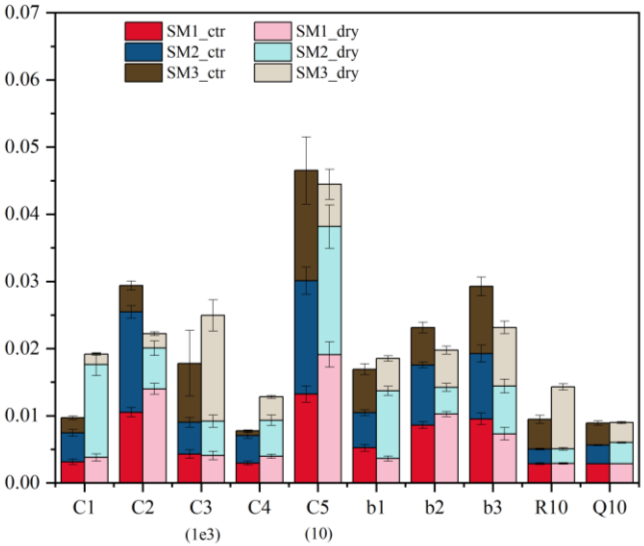

Figure A3. Maximum likelihood value (MLEs) (or means for unconstrained parameters) of the target parameters of vegetations in various models and treatments. Error bars represent standard deviations (SDs). See Table S1 for parameter abbreviations and units.

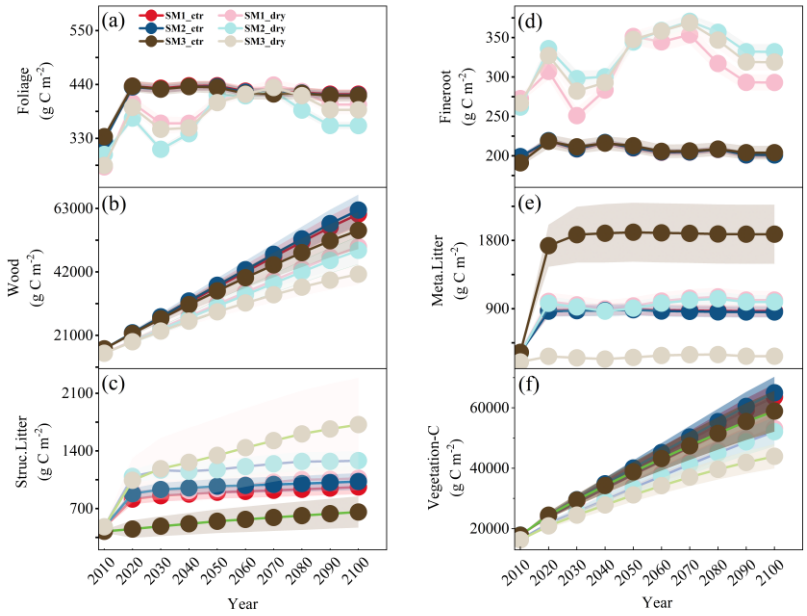

983

984 **Figure A4.** Predicted foliage (a), wood (b), structural litter (c), fineroot (d), Metabolic
985 litter (e), Vegetation C (f) from 2014 – 2100 under dry and control conditions for three
986 schemes.
987
988
989

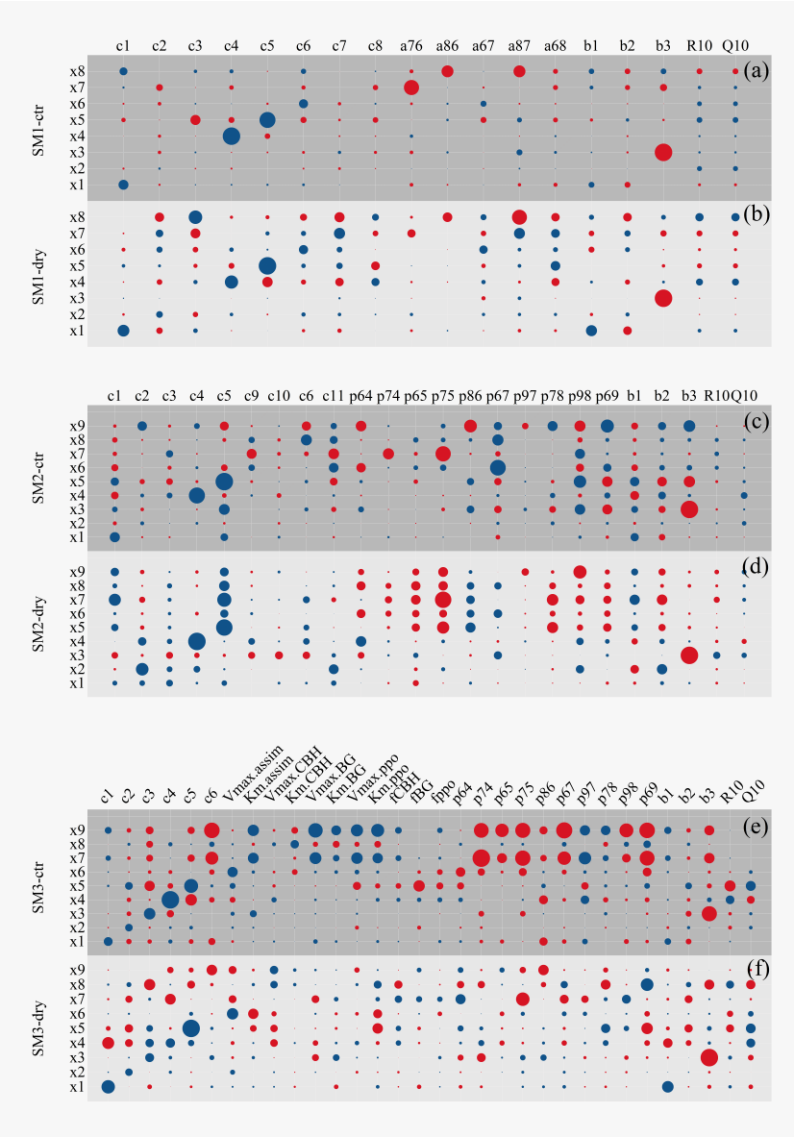

Figure A5. The correlation between carbon pools and model parameters under control and drought conditions of three schemes. Red represents positive correlation and blue represents negative correlation. The *x1, x2, x3, x4, x5* represent the carbon content of foliage, fineroot, wood, metabolic litter, structural litter. *x6, x7, x8* represent microbes slow SOM and passive SOM for SM1. *x6, x7, x8, x9* represent DOC, POC, microbes and MAOC for SM2 and SM3.

998

999 **Table A1.** Target parameters of this study and their prior ranges.

Parameters	Intervals	Unit	Description
C1	0.176-9.95	mg C g^{-1} d^{-1}	exit rate of C from foliage
C2	0.176-17.9	mg C g^{-1} d^{-1}	exit rate of C from fineroot
C3	0.00176-0.01	mg C g^{-1} d^{-1}	exit rate of C from wood
C4	0.274-8.22	mg C g^{-1} d^{-1}	exit rate of C from metabolic litter
C5	0.0548-1.64	mg C g^{-1} d^{-1}	exit rate of C from structural litter
C6	2.74-13.7	mg C g^{-1} d^{-1}	exit rate of C from microbes
C7	0.027-1.37	mg C g^{-1} d^{-1}	exit rate of C from slow SOM
C8	0.00137-0.00913	mg C g^{-1} d^{-1}	exit rate of C from passive SOM
C9	2.74-68.5	mg C g^{-1} d^{-1}	exit rate of C from DOC
C10	0.1-1	mg C g^{-1} d^{-1}	exit rate of C from POC
C11	0.00137-0.013	mg C g^{-1} d^{-1}	exit rate of C from MAOC
b1	0-0.315	-	allocation of GPP to foliage
b2	0-0.3	-	allocation of GPP to fineroot
b3	0-0.3	-	allocation of GPP to wood
R10	0-1	g C m^{-2} d^{-1}	basic respiration rate
Q10	2-5	-	temperature sensitivity of respiration
a76	0-0.5	-	allocation of microbes to slow SOM
a86	0-0.5	-	allocation of microbes to passive SOM
a67	0-0.5	-	allocation of slow SOM to microbes
a87	0-0.5	-	allocation of slow SOM to passive SOM
a68	0-1	-	allocation of passive SOM to microbes
p64	0-0.3	-	allocation of metabolic litter to DOC
p74	0-0.7	-	allocation of metabolic litter to POC
p65	0-0.6	-	allocation of structural litter to DOC
p75	0-0.4	-	allocation of structural litter to POC
p86	0-0.7	-	allocation of DOC to microbes

$p67$	0-0.8	-	allocation of POC to DOC
$p97$	0-0.2	-	allocation of POC to MAOC
$p78$	0-0.7	-	allocation of microbes to POC
$p98$	0-0.3	-	allocation of microbes to MAOC
$p69$	0-0.8	-	allocation of MAOC to DOC
$V_{max.assim}$	0.001-0.4	mg C mg^{-1} MBC d^{-1}	microbe maximum assimilation rate
$Km_{.assim}$	300-3000	g C m^{-3}	half-saturation for assimilation
$V_{max.CBH}$	0.0001-0.01	mg C mg^{-1} CBH d^{-1}	maximum reaction rate of CBH
$Km_{.CBH}$	300-3000	g C m^{-3}	half-saturation for reaction of CBH
$V_{max.PPO}$	0.0001-0.2	mg C mg^{-1} PPO d^{-1}	maximum reaction rate of PPO
$Km_{.PPO}$	300-6000	g C m^{-3}	half-saturation for reaction of PPO
$V_{max.BG}$	0.0001-0.2	mg C mg^{-1} BG d^{-1}	maximum reaction rate of BG
$Km_{.BG}$	300-3000	g C m^{-3}	half-saturation for reaction of BG
f_{CBH}	0-0.01	-	CBH-to-microbial carbon ratio
f_{PPO}	0-0.2	-	PPO-to-microbial carbon ratio
f_{BG}	0-0.1	-	BG-to-microbial carbon ratio

1000

1001

References

Abramoff, R. Z., Guenet, B., Zhang, H. C., Georgiou, K., Xu, X. F., Rossel, R. A. V., Yuan, W. P., and Ciais, P.: Improved global-scale predictions of soil carbon stocks with Millennial Version 2, Soil Biol Biochem., 164, https://doi.org/10.1016/j.soilbio.2021.108466, 2022.

Anderegg, WRL., Trugman, AT., Badgley, G., Konings, AG., and Shaw, J.: Divergent forests sensitivity to repeated extreme droughts, Nat. Clim. Change., 10(12), 1091-U19, https://doi.org/10.1038/s41558-020-00919-1, 2020.

Allison, S. D.: Microbial drought resistance may destabilize soil carbon, Trends Microbiol., 31(8), 780-787, https://doi.org/10.1016/j.tim.2023.03.002, 2023.

Allison, S. D., and Martiny, J. B. H.: Resistance, resilience, and redundancy in microbial communities, PNAS., 105, 11512-11519, https://doi.org/10.1073/pnas.0801925105, 2008.

Allison, S. D., Wallenstein, M. D., and Bradford, M. A.: Soil-carbon response to warming dependent on microbial physiology, Nat. Geosci., 3(5), 336-340, https://doi.org/10.1038/NGEO846, 2010.

Basile-Doelsch, I., Balesdent, J., and Pellerin, S.: Reviews and syntheses: The mechanisms underlying carbon storage in soil, BIOGEOSCIENCES., 17(21), 5223- 5242, https://doi.org/10.5194/bg-17-5223-2020, 2020.

Bastida, F., Torres, I. F., Andrés-Abellán, M., Baldrian, P., López-Mondéjar, R., Vetrovsky, T., and Jehmlich, N.: Differential sensitivity of total and active soil microbial communities to drought and forest management, Glob Chang Biol.., 24(1), 552-552, https://doi.org/10.1111/gcb.13953, 2018.

Benbi, D. K., Boparai, A. K., and Brar, K.: Decomposition of particulate organic matter is more sensitive to temperature than the mineral associated organic matter, Soil Biol Biochem., 70, 183-192, https://doi.org/10.1016/j.soilbio.2013.12.032, 2014.

Blankinship, JC., Fonte, SJ., Six, J., and Schimel, JP.: Plant versus microbial controls on soil aggregate stability in a seasonally dry ecosystem, GEODERMA., 272(39-50), https://doi.org/10.1016/j.geoderma.2016.03.008, 2016

Barnard, RL., Osborne, CA., and Firestone, MK.: Responses of soil bacterial and fungal communities to extreme desiccation and rewetting, ISME J.., 7(11), 2229-2241, https://doi.org/10.1038/ismej.2013.104, 2013.

Bu, X. L., Gu, X. Y., Zhou, X. Q., Zhang, M. Y., Zhang, M. Y., Zhang, J., Zhou, X. H., Chen, X. Y., and Wang, X. H.: Extreme drought slightly decreased soil labile organic C and N contents and altered microbial community structure in a subtropical evergreen forest, For. Ecol. Manage., 429, 18-27, https://doi.org/10.1016/j.foreco.2018.06.036, 2018.

Caldwell, B. A.: Enzyme activities as a component of soil biodiversity: A review, Pedobiologia., 49(6), 637-644, https://doi.org/10.1016/j.pedobi.2005.06.003, 2005.

Camino-Serrano, M., Guenet, B., Luyssaert, S., Ciais, P., Bastrikov, V., De Vos, B., Gielen, B., Gleixner, G., Jornet-Puig, A., Kaiser, K., Kothawala, D., Lauerwald,

设置了格式: 超链接, 字体: (默认) Times New Roman, 小四

设置了格式: 超链接, 字体: (默认) +西文正文 (等线), 五号

设置了格式: 超链接, 字体: (默认) Times New Roman, 小四

设置了格式: 超链接, 字体: (默认) +西文正文 (等线), 五号

设置了格式: 超链接, 字体: (默认) Times New Roman, 小四

设置了格式: 超链接, 字体: (默认) Times New Roman, 小四

删除了: Bach, E., Seger, GDD., Fernandes, GD., Lisboa, BB., and Passaglia, LMP.: Evaluation of biological control and rhizosphere competence of plant growth promoting bacteria, Appl. Soil. Ecol, 99(141-149), https://doi.org/10.1016/j.apsoil.2015.11.002, 2016.

设置了格式: 超链接, 字体: (默认) Times New Roman, 小四

设置了格式: 超链接, 字体: (默认) Times New Roman, 小四

设置了格式: 超链接, 字体: (默认) Times New Roman, 小四

设置了格式: 超链接, 字体: (默认) Times New Roman, 小四

设置了格式: 超链接, 字体: (默认) Times New Roman, 小四

R., Peñuelas, J., Schrumpf, M., Vicca, S., Vuichard, N., Walmsley, D., and Janssens, I. A.: ORCHIDEE-SOM: modeling soil organic carbon (SOC) and dissolved organic carbon (DOC) dynamics along vertical soil profiles in Europe, Geosci. Model Dev.., 11(3), 937-957, https://doi.org/10.5194/gmd-11-937-2018, 2018.

Campbell, C. A.: Soil organic carbon, nitrogen, and fertility, Dev. Soil Sci.., 8, 173-271, https://doi.org/10.1016/S0166-2481(08)70020-5, 1978.

Castro, H. F., Classen, A. T., Austin, E. E., Norby, R. J., and Schadt, C. W.: Soil Microbial Community Responses to Multiple Experimental Climate Change Drivers, Appl. Environ. Microbiol., 76(4), 999-1007, https://doi.org/10.1128/AEM.02874-09, 2010.

Chandel, A. K., Jiang, L. F., and Luo, L. Q.: Microbial Models for Simulating Soil Carbon Dynamics: A Review, J GEOPHYS RES- BIOGEO., 128(8), https://doi.org/10.1029/2023JG007436, 2023.

Chen, J., Luo, YQ., van Groenigen, KJ., Hungate, BA., Cao, JJ., Zhou, XH., and Wang, RW.: A keystone microbial enzyme for nitrogen control of soil carbon storage, Sci. Adv., 4(8), https://doi.org/10.1126/sciadv.aaq1689, 2018.

Choat, B., Brodribb, T. J., Brodersen, C. R., Duursma, R. A., López, R., and Medlyn, B. E.: Triggers of tree mortality under drought, NATURE., 558(7711), 531-539, https://doi.org/10.1038/s41586-018-0240-x, 2018.

Citerne, N., Wallace, H. M., Lewis, T., Reverchon, F., Omidvar, N., Hu, H. W., Shi, X. Z., Zhou, X. H., Zhou, G. Y., Farrar, M., Rashti, M. R., and Bai, S. H.: Effects of Biochar on Pulse C and N Cycling After a Short-term Drought: a Laboratory Study, J. Soil Sci. Plant Nutr.., 21(4), 2815-2825, https://doi.org/10.1007/s42729-021-00568-z, 2021.

Cotrufo, M. F., and Lavallee, J. M.: Soil organic matter formation, persistence, and functioning: A synthesis of current understanding to inform its conservation and regeneration, Adv. Agron., 172, 1-66, https://doi.org/10.1016/bs.agron.2021.11.002, 2022.

Cotrufo, M. F., Ranalli, M. G., Haddix, M. L., Six, J., and Lugato, E.: Soil carbon storage informed by particulate and mineral-associated organic matter, Nat. Geosci., 12(12), 989-994, https://doi.org/10.1038/s41561-019-0484-6, 2019.

Cotrufo, M. F., Wallenstein, M. D., Boot, C. M., Denef, K., and Paul, E.: The Microbial Efficiency-Matrix Stabilization (MEMS) framework integrates plant litter decomposition with soil organic matter stabilization: do labile plant inputs form stable soil organic matter? Glob Chang Biol.., 19(4), 988-95, https://doi.org/10.1111/gcb.12113, 2013.

de Vries, FT., Griffiths, RI., Bailey, M., Craig, H., Girlanda, M., Gweon, HS., Hallin, S., Kaisermann, A., Keith, AM., Kretzschmar, M., Lemanceau, P., Lumini, E., Mason, KE., Oliver, A., Ostle, N., Prosser, JI., Thion, C., Thomson, B., Bardgett, RD.: Soil bacterial networks are less stable under drought than fungal networks, Nat. Commun., 9, https://doi.org/10.1038/s41467-018-05516-7, 2018.

Du, F. F., Zhang, Y. M., Zhou, L. Y., Dietrich, P., Zhou, G. Y., Wang, J., Zhang, Q. Z., Wang, X. C., Du, Z. G., and Zhou, X. H.: Similar carbon accumulation rates with

设置了格式: 超链接, 字体: (默认) Times New Roman, 小四

设置了格式: 超链接, 字体: (默认) Times New Roman, 小四

设置了格式: 超链接, 字体: (默认) Times New Roman, 小四

设置了格式: 超链接, 字体: (默认) Times New Roman, 小四

设置了格式: 超链接, 字体: (默认) Times New Roman, 小四

删除了: Ciais, P., Reichstein, M., Viovy, N., Granier, A., Ogée, J., Allard, V., Aubinet, M., Buchmann, N., Bernhofer, C., Carrara, A., Chevallier, F., De Noblet, N., Friend, AD., Friedlingstein, P., Grünwald, T., Heinesch, B., Keronen, P., Knohl, A., Krinner, G., Loustau, D., Manca, G., Matteucci, G., Miglietta, F., Ourcival, JM., Papale, D., Pilegaard, K., Rambal, S., Seufert, G., Soussana, JF., Sanz, MJ., Schulze, ED., Vesala, T., and Valentini, R.: Europe-wide reduction in primary productivity caused by the heat and drought in 2003, NATURE., 437(7058), 529-333, https://doi.org/10.1038/nature03972, 2005.

设置了格式: 超链接, 字体: (默认) Times New Roman, 小四

设置了格式: 超链接, 字体: (默认) +西文正文 (等线), 五号

设置了格式: 超链接, 字体: (默认) Times New Roman, 小四

distinct drivers in two temperate forest restoration approaches, CATENA., 258, https://doi.org/10.1016/j.catena.2025.109249, 2025.

Du, Z. G., Nie, Y. Y., He, Y. H., Yu, G. R., Wang, H. M., and Zhou, X. H.: Complementarity of flux- and biometric-based data to constrain parameters in a terrestrial carbon model, TELLUS B., 67, https://doi.org/10.3402/tellusb.v67.24102, 2015.

Du, Z. G., Zhou, X. H., Shao, J. J., Yu, G. R., Wang, H. M., Zhai, D. P., Xia, J. Y., and Luo, YQ.: Quantifying uncertainties from additional nitrogen data and processes in a terrestrial ecosystem model with Bayesian probabilistic inversion, Adv. Model. Earth Syst., 9(1), 548-565, https://doi.org/10.1002/2016MS000687, 2017.

Eastman, B. A., Wieder, W. R., Hartman, M. D., Brzostek, E. R., Peterjohn, and W. T. Can models adequately reflect how long-term nitrogen enrichment alters the forest soil carbon cycle? BIOGEOSCIENCES., 21(1), 201-221, https://doi.org/10.5194/bg-21-201-2024, 2024.

Evans, C. D., Monteith, D. T., and Cooper, D. M.: Long-term increases in surface water dissolved organic carbon: Observations, possible causes and environmental impacts, Environ. Pollut., 137(1), 55-71, https://doi.org/10.1016/j.envpol.2004.12.031, 2005.

Ficken, C. D., and Warren, J. M.: The carbon economy of drought: comparing respiration responses of roots, mycorrhizal fungi, and free-living microbes to an extreme dry-rewet cycle, PLANT SOIL., 435(1-2), 407-422, https://doi.org/10.1007/s11104-018-03900-2, 2019.

Feng, J., Yao, Y., He, Y., Wang, P., Hu, H., and Zhang, S.: Hydraulic strategies of Cunninghamia lanceolata under drought are shaped by native drought conditions, For. Res., 5, e031, doi: https://doi.org/10.48130/forres-0025-0031. 2025.

Gao, Q., Hasselquist, N. J., Palmroth, S., Zheng, Z. M., and You, W. H.: Short-term response of soil respiration to nitrogen fertilization in a subtropical evergreen forest, Soil Biol Biochem., 76, 297-300, https://doi.org/10.1016/j.soilbio.2014.04.020, 2014.

Guo, X. W., Rossel, R. A. V., Wang, G. C., Xiao, L. J., Wang, M. M., Zhang, S., and Luo, Z. K.: Particulate and mineral-associated organic carbon turnover revealed by modelling their long-term dynamics, Soil Biol Biochem., 173, https://doi.org/10.1016/j.soilbio.2022.108780, 2022.

Han, Y. A., Deng, J. J., Zhou, W. M., Wang, Q. M., and Yu, D. P.: Seasonal Responses of Hydraulic Function and Carbon Dynamics in Spruce Seedlings to Continuous Drought, Front. Plant Sci., 13, https://doi.org/10.3389/fpls.2022.868108, 2022.

Hansen, P. M., Even, R., King, A. E., Lavallee, J., Schipanski, M., and Cotrufo, M. F.: Distinct, direct and climate-mediated environmental controls on global particulate and mineral-associated organic carbon storage, Glob Chang Biol., 30(1), https://doi.org/10.1111/gcb.17080, 2024.

Hao, X. C., and Singh, V. P.: Drought characterization from a multivariate perspective: A review, J. Hydrol., 527, (668-678), https://doi.org/10.1016/j.jhydrol.2015.05.031, 2015.

Honeker, L. K., Pugliese, G., Ingrisch, J., Fudyma, J., Gil-Loaiza, J., Carpenter, E.,

设置了格式: 超链接, 字体: (默认) Times New Roman, 小四

设置了格式: 超链接, 字体: (默认) Times New Roman, 小四

设置了格式: 超链接, 字体: (默认) Times New Roman, 小四

设置了格式: 超链接, 字体: (默认) Times New Roman, 小四

设置了格式: 超链接, 字体: (默认) Times New Roman, 小四

设置了格式: 超链接, 字体: (默认) Times New Roman, 小四

设置了格式: 超链接, 字体: (默认) Times New Roman, 小四

设置了格式: 超链接, 字体: (默认) Times New Roman, 小四

Singer, E., Hildebrand, G., Shi, L. L., Hoyt, D. W., Chu, R. K., Toyoda, J., Krechmer, J. E., Claflin, M. S., Ayala-Ortiz, C., Freire-Zapata, V., Pfannerstill, E. Y., Daber, L. E., Meeran, K., Dippold, M. A., Kreuzwieser, J., Williams, J., Ladd, S. N., Werner, C., Tfaily, M. M., and Meredith, L. K.: Drought re-routes soil microbial carbon metabolism towards emission of volatile metabolites in an artificial tropical rainforest, Nat. Microbiol.., 9(4), 1146-1147, https://doi.org/10.1038/s41564-023-01507-7, 2024.

Huang, Y., Guenet, B., Ciais, P., Janssens, I. A., Soong, J. L., Wang, Y. L., Goll, D., Blagodatskaya, E., and Huang, Y. Y.: ORCHIMIC (v1.0), a microbe-mediated model for soil organic matter decomposition, Geosci. Model Dev., 11(6), 2111-2138, https://doi.org/10.5194/gmd-11-2111-2018, 2018.

Hueso, S., García, C., and Hernández, T.: Severe drought conditions modify the microbial community structure, size and activity in amended and unamended soils, Soil Biol Biochem., 50(167-173), https://doi.org/10.1016/j.soilbio.2012.03.026, 2012.

IPCC, 2023: Climate Change 2023: Synthesis Report. Contribution of Working Groups I, II and III to the Sixth Assessment Report of the Intergovernmental Panel on Climate Change [Core Writing Team, H. Lee and J. Romero (eds.)]. IPCC, Geneva, Switzerland, pp. 35-115, doi: 10.59327/IPCC/AR6-9789291691647.

Jenny, H.: Factors of soil formation, McGraw-Hill, New York, 1941.

Jiang Z, Fu Y, Zhou L, He Y, Zhou G, Dietrich P, Long J, Wang X, Jia S, Ji Y, Jia Z, Song B, Liu R, Zhou X.: Plant growth strategy determines the magnitude and direction of drought-induced changes in root exudates in subtropical forests, Glob Chang Biol., 29, 3476-3488, 2023.

Knorr, W., Prentice, I. C., House, J. I., and Holland, E. A.: Long-term sensitivity of soil carbon turnover to warming, NATURE., 433(7023), 298-301, https://doi.org/10.1038/nature03226, 2005.

Krinner, G., Viovy, N., de Noblet-Ducoudré, N., Ogée, J., Polcher, J., Friedlingstein, P., Ciais, P., Sitch, S., and Prentice, I. C.: A dynamic global vegetation model for studies of the coupled atmosphere-biosphere system -: art. no. GB1015, Global Biogeochem. Cycles., 19(1), https://doi.org/10.1029/2003GB002199, 2005.

Lawrence, C. R., Neff, J. C., and Schimel, J. P.: Does adding microbial mechanisms of decomposition improve soil organic matter models? A comparison of four models using data from a pulsed rewetting experiment, Soil Biol Biochem., 41(9), 1923-1934, https://doi.org/10.1016/j.soilbio.2009.06.016, 2009.

Lawrence, D. M., Fisher, R. A., Koven, C. D., Oleson, K. W., Swenson, S. C., Bonan, G., Collier, N., Ghimire, B., van Kampenhout, L., Kennedy, D., Kluzek, E., Lawrence, P. J., Li, F., Li, H. Y., Lombardozzi, D., Riley, W. J., Sacks, W. J., Shi, M. J., Vertenstein, M., Wieder, W. R., Xu, C. G., Ali, A. A., Badger, A. M., Bisht, G., van den Broeke, M., Brunke, M. A., Burns, S. P., Buzan, J., Clark, M., Craig, A., Dahlin, K., Drewniak, B., Fisher, J. B., Flanner, M., Fox, A. M., Gentine, P., Hoffman, F., Keppel-Aleks, G., Knox, R., Kumar, S., Lenaerts, J., Leung, L. R., Lipscomb, W. H., Lu, Y. Q., Pandey, A., Pelletier, J. D., Perket, J., Randerson, J.

设置了格式: 超链接, 字体: (默认) Times New Roman, 小四

设置了格式: 超链接, 字体: (默认) Times New Roman, 小四

删除了: IPCC (intergovernmental Panel on Climate Change), *Climate Change 2013: the Physical Science Basis*, Cambridge University Press, Cambridge, UK, 2013

设置了格式: 超链接, 字体: (默认) Times New Roman, 小四

设置了格式: 超链接, 字体: (默认) Times New Roman, 小四

T., Ricciuto, D. M., Sanderson, B. M., Slater, A., Subin, Z. M., Tang, J. Y., Thomas, R. Q., Martin, M. V., and Zeng, X. B.: The Community Land Model Version 5: Description of New Features, Benchmarking, and Impact of Forcing Uncertainty. J. Adv. Model. Earth Syst, 11(12), 4245-4287. https://doi.org/10.1029/2018MS001583, 2019.

Lee, J., and Rossel, R. V. A.: Soil carbon simulation confounded by different pool initialization, Nutr. Cycling Agroecosyst., 116(2), 245-255, https://doi.org/10.1007/s10705-019-10041-0, 2020.

Liang, C., Kästner, M., and Joergensen, R. G.: 2020. Microbial necromass on the rise: The growing focus on its role in soil organic matter development. Soil Biol Biochem, 150, https://doi.org/1016/j.soilbio.2020.108000, 2020.

Lugato, E., Lavallee, JM., Haddix, ML., Panagos, P., Cotrufo, MF.: 2022. Different climate sensitivity of particulate and mineral-associated soil organic matter. Nat. Geosci., 15(6), 509-509, https://doi.org/10.1038/s41561-022-00945-y, 2022.

Luo, Z. K., Luo, Y. Q., Wang, G. C., Xia, J. Y., and Peng, C. H.: Warming-induced global soil carbon loss attenuated by downward carbon movement. Glob Chang Biol., 26(12), 7242-7254, https://doi.org/10.1111/gcb.15370, 2020.

Martiny, J. B. H., Jones, S. E., Lennon, J. T., and Martiny, A. C.: Microbiomes in light of traits: A phylogenetic perspective, SCIENCE., 350(6261), https://doi.org/10.1126/science.aac9323, 2015.

Meir, P., Metcalfe, D. B., Costa, A. C. L., and Fisher, R. A.: The fate of assimilated carbon during drought: impacts on respiration in Amazon rainforests, PHILOS T R SOC B., 363(1498), 1849-1855, https://doi.org/10.1098/rstb.2007.0021, 2008.

Moorhead, D. L., Sinsabaugh, R. L.: A theoretical model of litter decay and microbial interaction, Ecol. Monogr., 76(2), 151-174, https://doi.org/10.1890/0012-9615(2006)076[0151:ATMOLD]2.0.CO;2, 2006.

Müller, L. M., and Bahn, M.: Drought legacies and ecosystem responses to subsequent drought, Glob Chang Biol., 28(17), 5086-5103. https://doi.org/10.1111/gcb.16270, 2022.

Paul, E. A., and Van Vee, J. A.: The use of tracers to determine the dynamic nature of organic matter, Trans. Int. Congr. Soil Sci., 11(3), 61-102, 1978.

Pennisi, E.: Global drought experiment reveals the toll on plant growth, Science., 377(6609), 901-910, https://doi.org/10.1126/science.ade5540.Epub 2022 Aug 25, 2022.

Preece, C., Verbruggen, E., Liu, L., Weedon, J. T., and Peñuelas, J.: Effects of past and current drought on the composition and diversity of soil microbial communities, Soil Biol Biochem., 131(28-39), https://doi.org/10.1016/j.soilbio.2018.12.022, 2019.

Quiroga, G., Castagneyrol, B., Abdala-Roberts, L., and Moreira, X.: A meta-analysis of the effects of climate change-related abiotic factors on aboveground and belowground plant-associated microbes, OIKOS., 2024(7), https://doi.org/10.1111/oik.10411, 2024.

Reinelt, L., Whitaker, J., Kazakou, E., Bonnal, L., Bastianelli, D., Bullock, JM., Ostle, NJ.: Drought effects on root and shoot traits and their decomposability, Funct.Ecol.,

设置了格式: 超链接, 字体: (默认) Times New Roman, 小四

删除了: 。

设置了格式: 超链接, 字体: (默认) Times New Roman, 小四

设置了格式: 字体: (默认) Times New Roman, 小四

设置了格式: 超链接, 字体: (默认) Times New Roman, 小四

设置了格式: 超链接, 字体: (默认) Times New Roman, 小四

设置了格式: 超链接, 字体: (默认) Times New Roman, 小四

设置了格式: 字体: 小四

设置了格式: 超链接, 字体: (默认) Times New Roman, 小四

设置了格式: 超链接, 字体: (默认) +西文正文 (等线), 五号

设置了格式: 超链接, 字体: (默认) Times New Roman, 小四

37(4), 1044-1054, https://doi.org/10.1111/1365-2435.14261, 2023.
Ricks, K. D., and Yannarell, A. C.: Soil moisture incidentally selects for microbes that facilitate locally adaptive plant response, P ROY SOC B-BIOL SCI., 290(2001), https://doi.org/10.1098/rspb.2023.0469, 2023.
Rowland, L., Ramírez-Valiente, J. A., Hartley, I. P., and Mencuccini, M.: How woody plants adjust above- and below-ground traits in response to sustained drought, New Phytol., 239(4), 1173-1189, https://doi.org/10.1111/nph.19000, 2023.
Saiya-Cork, K. R., Sinsabaugh, R. L., and Zak, D. R.: The effects of long term nitrogen deposition on extracellular enzyme activity in an Acer Saccharum forest soil, Soil Biol Biochem., 34(9), 1309-1315, https://doi.org/10.1016/S0038-0717(02)00074-3, 2002.
Sardans, J., and Peñuelas, J.: Soil Enzyme Activity in a Mediterranean Forest after Six Years of Drought, Soil Sci. Soc. Am. J., 74(3), 838-851, https://doi.org/10.2136/sssaj2009.0225, 2010.
Schimel, J. P.: Life in Dry Soils: Effects of Drought on Soil Microbial Communities and Processes, ANNU REV ECOL EVOL S., 49, 409-432, https://doi.org/10.1146/annurev-ecolsys-110617-062614, 2018.
Schwalm, C. R., Anderegg, W. R. L., Michalak, A. M., Fisher, J. B., Biondi, F., Koch, G., Litvak, M., Ogle, K., Shaw, J. D., Wolf, A., Huntzinger, D. N., Schaefer, K., Cook, R., Wei, Y. X., Fang, Y. Y., Hayes, D., Huang, M. Y., Jain, A., and Tian, H. Q.: Global patterns of drought recovery, NATURE., 548(7666), 202-205, https://doi.org/10.1038/nature23021, 2017.
Si, Q., Chen, K., Wei, B., Zhang, Y., Sun, X., and Liang, J.: Formation of particulate organic carbon from dissolved substrate input enhances soil carbon sequestration, EGUsphere., https://doi.org/10.5194/egusphere-2023-1483, 2023.
Sokol, N. W., Sanderman, J., and Bradford, M. A.: Pathways of mineral-associated soil organic matter formation: Integrating the role of plant carbon source, chemistry, and point of entry, Glob Chang Biol., 25(1), 12-24, https://doi.org/10.1111/gcb.14482, 2019.
Sowerby, A., Emmett, B. A., Williams, D., Beier, C., and Evans, C. D.: The response of dissolved organic carbon (DOC) and the ecosystem carbon balance to experimental drought in a temperate shrubland, Eur. J. Soil Sci.., 61(5), 697-709, https://doi.org/10.1111/j.1365-2389.2010.01276.x, 2010.
Stursová, M., Zifcáková, L., Leigh, M. B., Burgess, R., and Baldrian, P.: Cellulose utilization in forest litter and soil: identification of bacterial and fungal decomposers, FEMS Microbiol. Ecol.., 80(3), 735-746, https://doi.org/10.1111/j.1574-6941.2012.01343.x, 2012.
Su, X., Su, X. L., Yang, S. C., Zhou, G. Y., Ni, M. Y., Wang, C., Qin, H., Zhou, X. H., and Deng, J.: Drought changed soil organic carbon composition and bacterial carbon metabolizing patterns in a subtropical evergreen forest, Sci. Total Environ., 736, https://doi.org/10.1016/j.scitotenv.2020.139568, 2020a.
Su, X. L., Su, X., Zhou, G. Y., Du, Z. G., Yang, S. C., Ni, M. Y., Qin, H., Huang, Z. Q., Zhou, X. H., and Deng, J.: Drought accelerated recalcitrant carbon loss by

设置了格式: 超链接, 字体: (默认) Times New Roman, 小四
设置了格式: 超链接, 字体: (默认) Times New Roman, 小四
设置了格式: 超链接, 字体: (默认) Times New Roman, 小四
设置了格式: 超链接, 字体: (默认) Times New Roman, 小四
设置了格式: 超链接, 字体: (默认) Times New Roman, 小四
设置了格式: 超链接, 字体: (默认) Times New Roman, 小四
设置了格式: 超链接, 字体: (默认) Times New Roman, 小四
设置了格式: 超链接, 字体: (默认) +西文正文 (等线), 五号
设置了格式: 超链接, 字体: (默认) Times New Roman, 小四

changing soil aggregation and microbial communities in a subtropical forest, Soil Biol Biochem., 148, https://doi.org/10.1016/j.soilbio.2020.107898, 2020b.

Szejgis, J., Carrillo, Y., Jeffries, T. C., Dijkstra, F. A., Chieppa, J., Horn, S., Bristol, D., Maisnam, P., Eldridge, D., and Nielsen, U. N.: Altered rainfall greatly affects enzyme activity but has limited effect on microbial biomass in Australian dryland soils, Soil Biol Biochem., 189, https://doi.org/10.1016/j.soilbio.2023.109277, 2024.

Tiwari, T., Sponseller, R., and Laudon, H.: The emerging role of drought as a regulator of dissolved organic carbon in boreal landscapes, Nat. Commun., 13(1), https://doi.org/10.1038/s41467-022-32839-3, 2022.

Tao, F., Houlton, B. Z., Huang, Y. Y., Wang, Y. P., Manzoni, S., Ahrens, B., Mishra, U., Jiang, L. F., Huang, X. M., and Luo, Y. Q.: Convergence in simulating global soil organic carbon by structurally different models after data assimilation, Glob Chang Biol., 30(5), https://doi.org/10.1111/gcb.17297, 2024.

Ulrich, DEM., Clendinen, CS., Alongi, F., Mueller, RC., Chu, RK., Toyoda, J., Gallegos-Graves, L., Goemann, HM., Peyton, B., Sevanto, S., Dunbar, J.: Root exudate composition reflects drought severity gradient in blue grama (Bouteloua gracilis), Sci.Rep., 12(1), https://doi.org/10.1038/s41598-022-16408-8, 2022.

Villarino, S. H., Pinto, P., Jackson, R. B., and Piñeiro, G.: Plant rhizodeposition: A key factor for soil organic matter formation in stable fractions, Sci Adv., 7(16), https://doi.org/10.1126/sciadv.abd3176, 2021.

Wan, F., Bian, C., Weng, E., Luo, Y., and Xia, J.: TECO-CNP Sv1.0: A coupled carbon-nitrogen-phosphorus model with data assimilation for subtropical forests, EGUsphere., https://doi.org/10.5194/egusphere-2025-1243, 2025.

Wang, XY., Lu, DL., Schonbeck, L., Han, YN., Bai, SB., Yu, DP., Han, QM., and Wang, QW.: Contrasting effects of prolonged drought and nitrogen addition on growth and non-structural carbohydrate dynamics in coexisting Pinus koraiensis and Fraxinus mandshurica saplings, For. Res., 5, e003, https://doi.org/10.48130/forres-0025-0002, 2025.

Wang, X, Zhou, L, Fu, Y, Jiang, Z, Jia, S, Song, B, Liu, D, and Zhou, X.: Drought-induced changes in rare microbial community promoted contribution of microbial necromass C to SOC in a subtropical forest, Soil Biol Biochem., 189, https://doi.org/10.1016/j.soilbio.2023.109252, 2024.

Williams, A., de Vries, FT.: Plant root exudation under drought: implications for ecosystem functioning, New Phytol., 225(5), 1899-1905, https://doi.org/10.1111/nph.16223, 2020.

Willard, S. J., Liang, G. P., Adkins, S., Foley, K., Murray, J., and Waring, B.: Land use drives the distribution of free, physically protected, and chemically protected soil organic carbon storage at a global scale, Glob Chang Biol., 30(9), https://doi.org/10.1111/gcb.17507, 2024.

Wu, H., Peng, C., Moore, T. R., Hua, D., Li, C., Zhu, Q., Peichl, M., Arain, MA., and Guo, Z.: Modeling dissolved organic carbon in temperate forest soils: TRIPLEX-DOC model development and validation. Geosci. Model Dev., 7(3), 867-881, https://doi.org/10.5194/gmd-7-867-2014, 2014.

设置了格式: 超链接, 字体: (默认) Times New Roman, 小四

设置了格式: 超链接, 字体: (默认) Times New Roman, 小四

设置了格式: 超链接, 字体: (默认) Times New Roman, 小四

设置了格式: 超链接, 字体: (默认) +西文正文 (等线), 五号

设置了格式: 超链接, 字体: (默认) Times New Roman, 小四

设置了格式: 超链接, 字体: (默认) Times New Roman, 小四

删除了: Waldrop, M. P., and Firestone, M. K.: Seasonal dynamics of microbial community composition and function in oak canopy and open grassland soils, Microb. Ecol., 52(3), 470-479, https://doi.org/10.1007/s00248-006-9100-6, 2006.

设置了格式: 超链接, 字体: (默认) Times New Roman, 小四

设置了格式: 超链接, 字体: (默认) +西文正文 (等线), 五号

Wu, R. Q., Wang, Y. S., Huo, X. Y., Chen, W. J., and Wang, D. X.: Drought and vegetation restoration patterns shape soil enzyme activity and nutrient limitation dynamics in the loess plateau, J. Environ. Manage., 374. https://doi.org/10.1016/j.jenvman.2024.123846, 2025.

Wu, J. F., Yao, H. X., Chen, X. H., and Chen, X. W.: Dynamics of dissolved organic carbon during drought and flood events: A phase-by-stages perspective, Sci. Total Environ., 871, https://doi.org/10.1016/j.scitotenv.2023.162158, 2023.

Wu, XW., Luo, YQ., Weng, ES., White, L., Ma, Y., Zhou, XH.: Conditional inversion to estimate parameters from eddy-flux observations, J. Plant Ecol., 2(2), 55-68, https://doi.org/10.1093/jpe/rtp005, 2009.

Xu, T., White, L., Hui, D. F., and Luo, Y. Q.: Probabilistic inversion of a terrestrial ecosystem model: Analysis of uncertainty in parameter estimation and model prediction, Global Biogeochem. Cycles., 20(2), https://doi.org/10.1029/2005GB002468, 2006.

Yin, H., Zheng, H. W., Zhang, B., Tariq, A., Lv, G. H., Zeng, F. J., and Graciano, C.: Stoichiometry of C: N: P in the Roots of Alhagi sparsifolia Is More Sensitive to Soil Nutrients Than Aboveground Organs, Frontiers in Plant Science, 12. https://doi.org/10.3389/fpls.2021.698961. 2021.

Zhao, T. H., Yang, X., He, R., Shi, B. K., Gao, W. F., Ma, J. Y., and Sun, W.: Plant-soil microbe adaptive strategies reshape soil respiration components under multi-year precipitation frequency reduction and nitrogen addition in a semi-arid grassland, Funct. Ecol.., 39(9), 2370-2380, https://doi.org/10.1111/1365-2435.70118, 2025.

Zhou, G. Y., Zhou, X. H., Liu, R. Q., Du, Z. G., Zhou, L. Y., Li, S. S., Liu, H. Y., Shao, J. J., Wang, J. W., Nie, Y. Y., Gao, J., Wang, M. H., Zhang, M. Y., Wang, X. H., and Bai, S. H.: Soil fungi and fine root biomass mediate drought-induced reductions in soil respiration, Funct. Ecol., 34(12), 2634-2643, https://doi.org/10.1111/1365-2435.13677, 2020.

Zhou, X. Q., Chen, C. R., Wang, Y. F., Xu, Z. H., Duan, J. C., Hao, Y. B., and Smaill, S.: Soil extractable carbon and nitrogen, microbial biomass and microbial metabolic activity in response to warming and increased precipitation in a semiarid Inner Mongolian grassland, GEODERMA., 206, 24-31 https://doi.org/10.1016/j.geoderma.2013.04.020, 2013.

设置了格式: 超链接, 字体: (默认) Times New Roman, 小四

删除了: Shi, Z., Crowell, S., Luo, YQ., and Moore, B.: Model structures amplify uncertainty in predicted soil carbon responses to climate change, Nat. Commun., 9, https://doi.org/10.1038/s41467-018-04526-9, 2018.

设置了格式: 超链接, 字体: (默认) Times New Roman, 小四